

# Resident and recruited macrophages differentially contribute to cardiac healing after myocardial ischemia

## Reviewed Preprint

Revised by authors after peer review.

[About eLife's process](#)


**Reviewed preprint version 3**  
March 4, 2024 (this version)

**Reviewed preprint version 2**  
January 19, 2024

**Reviewed preprint version 1**  
August 2, 2023

**Posted to preprint server**  
June 19, 2023

**Sent for peer review**  
June 9, 2023

**Tobias Weinberger, Denise Messerer, Markus Joppich, Max Fischer, Clarisabel Garcia, Konda Kumaraswami, Vanessa Wimpler, Sonja Ablinger, Saskia Räuber, Jiahui Fang, Lulu Liu, Wing Han Liu, Julia Winterhalter, Johannes Lichti, Lukas Tomas, Dena Esfandyari, Guelce Percin, Sandra Martin Salamanca, Andres Hidalgo, Claudia Waskow, Stefan Engelhardt, Andrei Todica, Ralf Zimmer, Clare Pridans, Elisa Gomez-Perdiguero, Christian Schulz** 

Medical Clinic I., Department of Cardiology, University Hospital, Ludwig Maximilian University, 81377 Munich, Germany • Institute of Surgical Research at the Walter-Brendel-Centre of Experimental Medicine, University Hospital, Ludwig Maximilian University, 81377 Munich, Germany • DZHK (German Centre for Cardiovascular Research), partner site Munich Heart Alliance, 80336 Munich, Germany • Institut Pasteur, Unité Macrophages et Développement de l'Immunité, Département de Biologie du Développement et Cellules Souches, Paris, France • LFE Bioinformatik, Department of Informatics, Ludwig Maximilian University, 80333 Munich, Germany • Department of Neurology, Medical Faculty, Heinrich Heine University of Düsseldorf, 40225 Düsseldorf, Germany • Institute of Pharmacology and Toxicology, Technical University Munich, 80802 Munich, Germany • Immunology of Aging, Leibniz-Institute on Aging - Fritz-Lipmann-Institute (FLI), 07745 Jena, Germany • Area of Cell & Developmental Biology, Centro Nacional de Investigaciones Cardiovasculares Carlos III, Madrid, Spain • Vascular Biology and Therapeutics Program and Department of Immunobiology, Yale University School of Medicine, New Haven, CT, USA • Faculty of Biological Sciences, Friedrich-Schiller-University, 07737 Jena, Germany • Department of Nuclear Medicine, Ludwig Maximilian University, 81377 Munich, Germany • University of Edinburgh Centre for Inflammation Research, The Queen's Medical Research Institute, Edinburgh EH16 4TJ, United Kingdom • Simons Initiative for the Developing Brain, Centre for Discovery Brain Sciences, University of Edinburgh, Edinburgh EH8 9XD, United Kingdom

 [https://en.wikipedia.org/wiki/Open\\_access](https://en.wikipedia.org/wiki/Open_access)

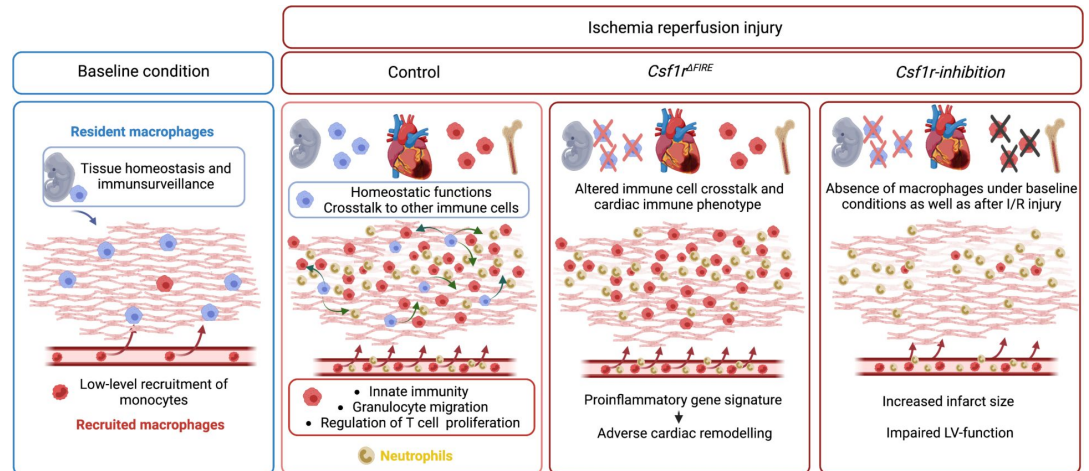
 Copyright information

## Abstract

Cardiac macrophages are heterogenous in phenotype and functions, which has been associated with differences in their ontogeny. Despite extensive research, our understanding of the precise role of different subsets of macrophages in ischemia/reperfusion injury remains incomplete. We here investigated macrophage lineages and ablated tissue macrophages in homeostasis and after I/R injury in a CSF1R-dependent manner. Genomic deletion of a *fms*-intronic regulatory element (FIRE) in the *Csf1r* locus resulted in specific absence of resident homeostatic and antigen-presenting macrophages, without affecting the recruitment of monocyte-derived macrophages to the infarcted heart. Specific absence of homeostatic, monocyte-independent macrophages altered the immune cell crosstalk in response to injury and induced proinflammatory neutrophil polarization, resulting in impaired cardiac remodelling without influencing infarct size. In contrast, continuous CSF1R inhibition led to depletion of both resident and recruited macrophage populations. This augmented adverse remodelling after I/R and led to an increased infarct size and deterioration of cardiac function. In summary, resident macrophages orchestrate inflammatory responses improving cardiac remodelling, while recruited macrophages

determine infarct size after I/R injury. These findings attribute distinct beneficial effects to different macrophage populations in the context of myocardial infarction.

## Graphical abstract



### eLife assessment

Using state-of-the-art fate-mapping models and genetic and pharmacological targeting approaches, this study provides **important** findings on the distinct functions exerted by resident and recruited macrophages during cardiac healing after myocardial ischemia. Evidence supporting the conclusions are **solid** with the use of the FIRE mouse model in combination with fate-mapping to target fetal-derived macrophages. This study will be of interest for the macrophage biologists working in the heart but also in others tissues in the context of inflammation.

## Introduction

Macrophages are important effectors of innate immunity. They are essential for host defense against infections but are also involved in different cardiovascular diseases. They represent the most abundant immune cell population in healthy cardiovascular tissues (Heidt *et al.*, 2014; Weinberger *et al.*, 2020), where they contribute to organ functions (Hulsmans *et al.*, 2017) and maintenance of tissue homeostasis (Nicolas-Avila *et al.*, 2020). In cardiovascular diseases such as atherosclerosis and its main sequelae, ischemic stroke and acute myocardial infarction (AMI), macrophage functions are central to both disease development and healing. AMI has remained a leading cause of mortality and morbidity worldwide (Ahmad & Anderson, 2021; Lozano *et al.*, 2012). Although acute survival in this condition has improved through the broad availability of percutaneous coronary intervention, adverse myocardial remodeling and fibrosis frequently result in heart failure (Gerber *et al.*, 2016). Pathophysiologically, the diminished blood supply to myocardial tissue during AMI leads to acute tissue necrosis, which induces a profound sterile inflammation and triggers complex cascade of immune processes and tissue remodeling (Hilgendorf *et al.*, 2014; Honold & Nahrendorf, 2018; Nahrendorf *et al.*, 2007). Consequently, uncontrolled immune reactions in the course of AMI are associated with impaired wound healing and adverse remodeling and can result in worsened cardiac outcome (Panizzi *et al.*, 2010).

Macrophages play an essential role in cardiac injury, and thus represent a potential therapeutic target (Hilgendorf *et al.*, 2014 [↗](#); Nahrendorf *et al.*, 2007 [↗](#)). However, they are an heterogeneous population (Kubota *et al.*, 2019 [↗](#); Weinberger & Schulz, 2015 [↗](#); Zaman & Epelman, 2022 [↗](#)), and a large body of work has shown that they can have both pro- and anti-inflammatory functions. The differential roles of macrophage populations in AMI have remained incompletely understood. Cardiac macrophages can derive from embryonic and adult hematopoietic progenitors (Epelman *et al.*, 2014 [↗](#)). Fate mapping analyses have identified yolk sac (YS) erythro-myeloid progenitors (EMPs) as a principal source of cardiac macrophages in adult life (Ginhoux *et al.*, 2010 [↗](#)). However, limited labeling in inducible cre reporter systems have not allowed for precisely differentiating and quantifying developmental origins of cardiac macrophages. Further, targeting of these macrophages has been challenging (Frieler *et al.*, 2015 [↗](#); Ruedl & Jung, 2018 [↗](#)).

In this study, we investigated the cellular identity of cardiac macrophages in association with their developmental paths and their immune responses to ischemia/reperfusion (I/R) injury. By combining lineage tracing with single cell RNA sequencing, we provide an in-depth analysis of the differential functions of resident and recruited cardiac macrophages. We then harnessed mice with genomic deletion of the *fms*-intronic regulatory element (FIRE) (Rojo *et al.*, 2019 [↗](#)), that allowed us to specifically address populations of resident macrophages in the infarcted heart and compared them to mice, in which both recruited as well as resident macrophages are depleted by pharmacological inhibition of the CSF1R-signalling pathway. Using these approaches of selective macrophage depletion, we could attribute different beneficial functions to resident and also to recruited macrophages which impact differently on cardiac remodeling, infarct size and cardiac outcome.

## Results

### Absence of resident cardiac macrophages in *Csf1r*<sup>ΔFIRE</sup> mice

To quantify the contribution of YS EMPs to cardiac resident macrophages, we harnessed constitutive labeling in *Rank*<sup>Cre</sup>;*Rosa26*<sup>eYFP</sup> mice (Jacome-Galarza *et al.*, 2019 [↗](#); Mass *et al.*, 2016 [↗](#); Percin *et al.*, 2018 [↗](#)). ~80% of cardiac macrophages expressed YFP in hearts of 12 week-old animals, whereas blood monocytes were not labeled (Fig 1A [↗](#); Fig S1). EMP-derived microglia served as control confirming high efficiency of Cre-mediated recombination. In a comparative analysis, we traced fetal and adult definitive hematopoiesis in *Flt3*<sup>Cre</sup>*Rosa26*<sup>eYFP</sup> mice (Gomez Perdiguero *et al.*, 2015 [↗](#); Schulz *et al.*, 2012 [↗](#)), indicating that ~20% of cardiac macrophages derived from definitive HSC (Fig 1B [↗](#)). Thus, the majority of resident macrophages in the healthy heart is of early embryonic origin.

To determine the role of resident macrophages in the mouse heart, we generated *Rank*<sup>Cre</sup>*Rosa26*<sup>DTR</sup> mice that express the avian diphtheria toxin (DT) receptor in the EMP lineage, rendering them susceptible to DT-mediated ablation. Administration of a single DT dose, however, resulted in premature death of all mice (n=6) within 24 hours (Fig S2). The injected mice presented with a systemic inflammatory response syndrome (SIRS)-like phenotype, indicating that acute depletion of EMP-derived macrophages is not viable.

In *Csf1r*<sup>ΔFIRE</sup> mice, genetic deletion of the *fms*-intronic regulatory element (FIRE) in the first intron of the *Csf1r* gene leads to a selective absence of tissue macrophages without the developmental defects observed in *Csf1r*<sup>-/-</sup> mice (Munro *et al.*, 2020 [↗](#); Rojo *et al.*, 2019 [↗](#)). We first confirmed that cardiac macrophages in *Csf1r*<sup>ΔFIRE/ΔFIRE</sup> mice (further termed ΔFIRE) mice were reduced by ~90% and the number of monocytes and neutrophils was not altered (Fig 1C-G [↗](#)). We thus crossed the ΔFIRE animals with the YS EMP fate mapping line (*Rank*<sup>Cre</sup>*Rosa26*<sup>eYFP</sup> mice) and showed that the macrophages absent in ΔFIRE animals were EMP-derived macrophages (Fig 1E [↗](#)), thus offering a new model to investigate the role of resident macrophages in cardiac injury.

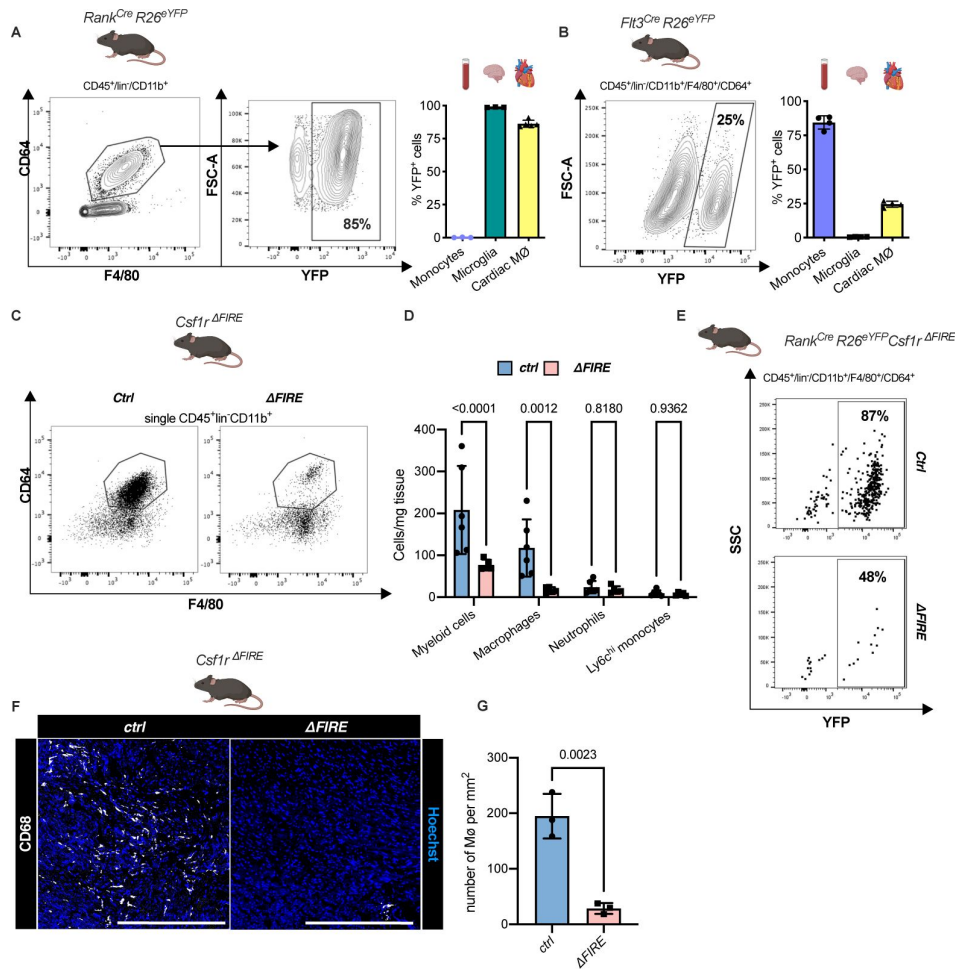


**Figure 1.**

### Absence of resident cardiac macrophages in *Csf1r<sup>ΔFIRE</sup>* mice.

(A) Flow cytometry analysis of 3 month-old *Rank<sup>Cre</sup>Rosa26<sup>eYFP</sup>* mice, showing single/CD45<sup>+</sup>/lin<sup>-</sup>(CD11c, Ter119, Tcrβ, Nk1.1)/CD11b<sup>+</sup> cardiac cells, eYFP expression in macrophages (CD64<sup>+</sup>/F4/80<sup>+</sup>) and percentage of eYFP<sup>+</sup> blood monocytes, microglia and cardiac macrophages (n=3-5 each from an independent experiment). (B) Flow cytometry analysis of 3 month-old *Flt3<sup>Cre</sup>Rosa26<sup>eYFP</sup>* mice, showing macrophage expression of eYFP and percentage of eYFP<sup>+</sup> blood monocytes, microglia and cardiac macrophages (n=4 each from an independent experiment). (C) Representative flow cytometry analysis of cardiac macrophages in *control* and *ΔFIRE* mice (D) Quantification of myeloid cells by flow cytometry (CD45<sup>+</sup>/lin<sup>-</sup>/CD11b<sup>+</sup>), macrophages (CD45<sup>+</sup>/lin<sup>-</sup>/CD11b<sup>+</sup>/CD64<sup>+</sup>/F4/80<sup>+</sup>), neutrophils (CD45<sup>+</sup>/lin<sup>-</sup>/CD11b<sup>+</sup>/CD64<sup>+</sup>/F4/80<sup>+</sup>/Ly6g<sup>+</sup>) and Ly6c<sup>hi</sup> monocytes (CD45<sup>+</sup>/lin<sup>-</sup>/CD11b<sup>+</sup>/CD64<sup>+</sup>/F4/80<sup>+</sup>/Ly6g<sup>+</sup>/Ly6c<sup>hi</sup>) (n=6 for *control* and n=5 for *ΔFIRE* mice, each single experiments). (E) Representative flow cytometry analysis of cardiac macrophages and their expression of eYFP in *Csf1r<sup>ΔFIRE/+</sup>Rank<sup>Cre</sup>Rosa26<sup>eYFP</sup>* and *Csf1r<sup>ΔFIRE/ΔFIRE</sup>Rank<sup>Cre</sup>Rosa26<sup>eYFP</sup>*. (F) Representative immunohistological images showing macrophages (CD68<sup>+</sup> cells in white and Hoechst in blue) in *control* and *ΔFIRE* hearts in 3 month-old mice at baseline conditions (scale bars represent 500μm). (F) Quantification of macrophages by histology ((n=3 for *control* and *ΔFIRE* mice). Either Fisher's LSD test or unpaired t-test were performed and mean ± SD is shown.

## Changes in the cardiac immune phenotype

### in *Csf1r*<sup>ΔFIRE</sup> mice in baseline conditions

To further characterize the macrophage populations absent in healthy hearts of adult ΔFIRE mice, we carried out single cell RNA-sequencing (scRNA-seq) of CD45<sup>+</sup> immune cells in wildtype, ΔFIRE and *Rank*<sup>Cre</sup>*Rosa26*<sup>eYFP</sup> mice (Fig 2A, Fig S3). We identified the presence of six macrophage clusters in control mice (Fig 2B, Fig S3). Two clusters of macrophages expressing homeostatic (e.g. *Lyve-1*, *Gas6*, *Stab1*) and antigen presentation-related genes (e.g. *CD74*, *H2-Ab1*) were specifically ablated in ΔFIRE mice (Fig 2C), which largely represent YFP-expressing macrophages in *Rank*<sup>Cre</sup>*Rosa26*<sup>eYFP</sup> mice (Fig 2D). Specifically, we mapped ~90% of *yfp* transcripts to the two clusters of homeostatic and antigen presenting macrophages that were ablated in ΔFIRE. Other clusters were not reduced in ΔFIRE, and also were not quantitatively represented in the YS macrophage lineage tracing model, i.e. *Cx3cr1*<sup>hi</sup>(2% *yfp*), *Ccr2*<sup>low</sup>*Ly6c*<sup>lo</sup> (5% *yfp*) and *Ccr2*<sup>hi</sup>*Ly6c*<sup>hi</sup> (1% *yfp*) macrophages within respective clusters (Fig 2D). The specific impact of ΔFIRE on resident macrophages is further supported by the observation, that no changes in gene expression nor cell numbers were observed in *Ly6c*<sup>hi</sup> monocytes and inflammatory *Ccr2*<sup>hi</sup>*Ly6c*<sup>hi</sup> macrophages (Fig 2C, Fig S4). Together, ΔFIRE allows for investigating the role of resident cardiac macrophages that are largely of YS origin.

Absence of resident macrophages in ΔFIRE was associated with changes in gene expression in non-macrophage clusters such as *T- and B-cells* and *natural killer (NK) cells* (Fig S5). Further, overall phagocytic capacity, as inferred by expression of phagocytosis related genes (Amorim *et al*, 2022), was reduced (Fig 2E). This suggests that absence of resident macrophages is accompanied by distinct changes in immune functions in the homeostatic heart.

### Adverse cardiac remodeling in *Csf1r*<sup>ΔFIRE</sup> mice after I/R injury

To assess the impact of the absence of resident macrophages in cardiac injury, we subjected ΔFIRE mice to I/R injury and investigated remodeling and functional outcome by sequential positron emission tomography (PET) imaging after 6 and 30 days (Fig 3A). Function of the cardiac left ventricle (LV), as determined by ejection fraction (LVEF) and stroke volume (SV), improved in controls in the course of post-I/R remodeling (Fig 3B-C). In contrast, LVEF and SV remained unchanged or worsened in ΔFIRE mice, and longitudinal observations of mice indicated a negative net effect on ejection fraction from day 6 to day 30 post I/R. Thus, absence of resident macrophages negatively influenced cardiac remodeling in the course of infarct healing (Fig 3D-G). Infarct size as determined by viability defect (PET) and fibrotic area (histology) was not different after 30 days (Fig 3E-H).

## Recruitment of BM-derived macrophages

### into infarct zone of *Csf1r*<sup>ΔFIRE</sup> mice

To gain a deeper understanding of the inflammatory processes taking place in the infarcted heart, we quantified macrophage distribution by immunofluorescence and flow cytometry analysis of ischemic and remote areas after I/R. In ΔFIRE mice, macrophages were largely absent in the remote zone of infarcted hearts (Fig 4A), indicating sustained depletion of resident macrophages. However, macrophages strongly increased in the infarct area and their numbers were not different in both infarct and border zones between ΔFIRE and control mice (Fig 4A). This indicated recruitment and differentiation of ΔFIRE-independent macrophages from the circulation into these regions. Indeed, complementing lineage tracing of BM HSC in *Flt3*<sup>Cre</sup> mice (Fig 4B) and YS EMP in *Rank*<sup>Cre</sup> mice (Fig 4C) proved the recruitment of macrophages from BM HSC (Flt3 GFP<sup>+</sup> and Rank RFP<sup>-</sup>, respectively) in the early phase of I/R injury. 30 days after I/R, BM-derived macrophages remained overrepresented in the infarct zone (~75% HSC contribution), and differential contribution of BM HSC declined from the border zone (~50%) to the remote zone

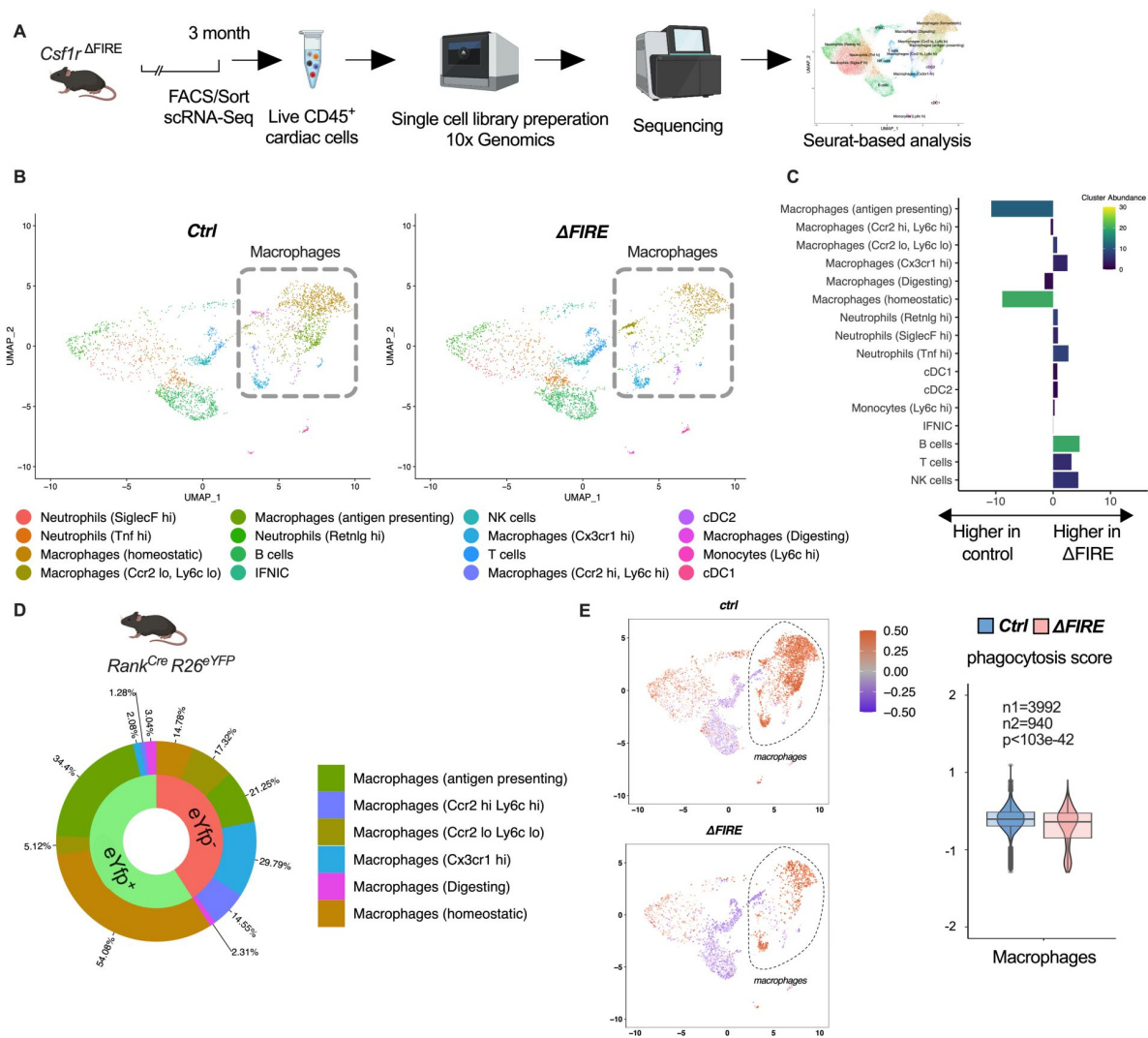


**Figure 2.**

**Changes in the cardiac immune phenotype in *Csf1*<sup>ΔFIRE</sup> mice in baseline conditions.**

(A) Experimental setup to analyze cardiac immune cells using scRNA-seq of sorted CD45<sup>+</sup>/live cells. (B) UMAPs of control and ΔFIRE in baseline conditions (n=3 for control and ΔFIRE) (C) Absolute difference (percentage points) in cluster abundance between control and ΔFIRE. (D) Contribution of EMP-derived (*eYfp* expressing) macrophages to the different macrophage clusters analysed by scRNA-seq analysis of immune cells harvested from a *Rank*<sup>Cre</sup>*Rosa26*<sup>eYFP</sup> mouse. (E) Phagocytosis score projected on a UMAP displaying control and ΔFIRE immune cell subsets. Violin and box plots show the computed phagocytosis score combined in all macrophage clusters (n1/n2 represents number of cells from control/ ΔFIRE mice).

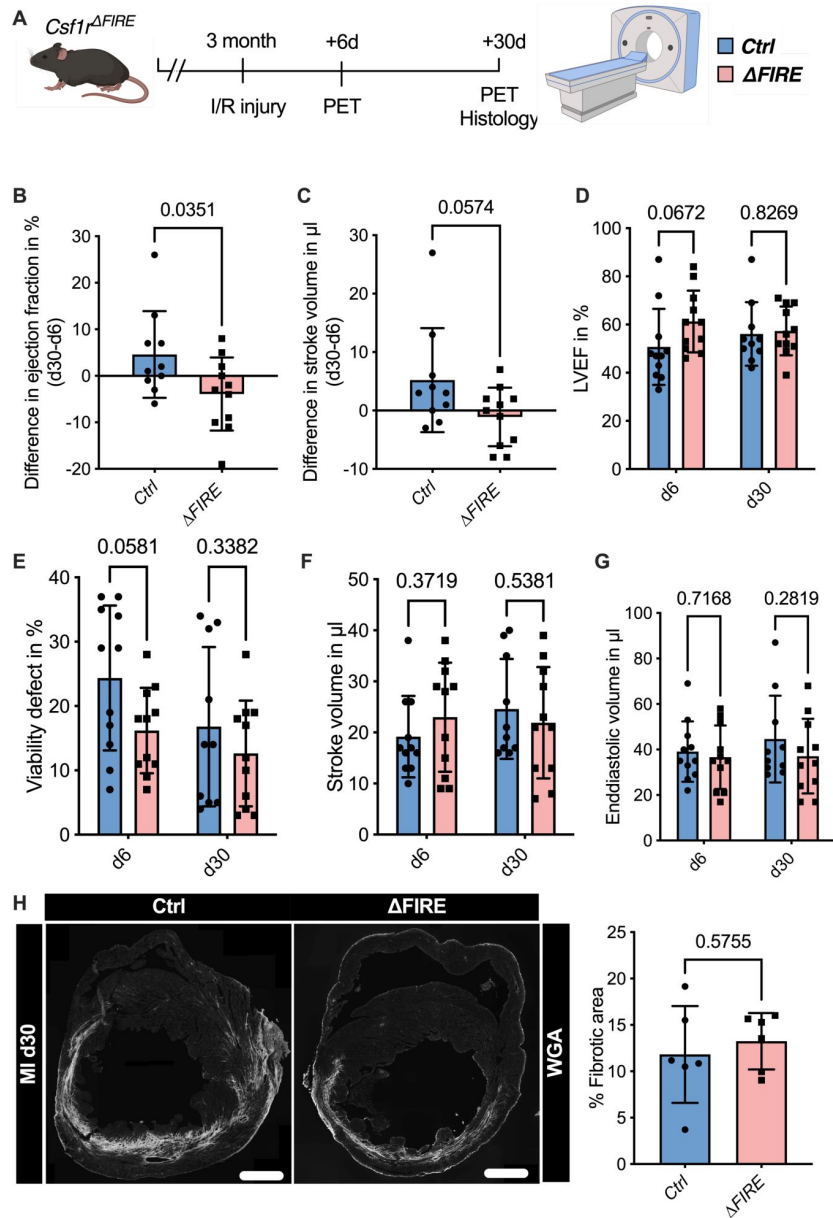


**Figure 3.**

### Adverse cardiac remodeling in *Csf1*<sup>ΔFIRE</sup> mice after I/R injury

(A) Schematic of the sequential analysis of cardiac function, dimensions and viability using positron-emission tomography 6 and 30 days after I/R injury in *control* and *ΔFIRE* with (B and C) showing the intraindividual changes in each parameter from d6 to d30 and (D-G) the individual timepoints on d6 and d30 (d6: n=11 for *control* and *ΔFIRE*, d30: n=10 for *control* and n=11 for *ΔFIRE*). (B and D) left ventricular ejection fraction (LVEF), (C and E) percentage of the viability defect, (F) stroke volume and (F) left-ventricular end-diastolic volume. (H) Representative immunohistological images showing the fibrotic area (WGA<sup>+</sup> area) in hearts from *control* and *ΔFIRE* mice 30 days after I/R injury. Right panel shows the percentage of fibrotic area in the respective groups (n= 6 for each group). Student's t-test was performed and mean  $\pm$  SD is shown.

(~35%) (**Fig 4D** [↗](#)). Taken together, recruited BM-derived macrophages represent the main population in the infarct area and their recruitment was unaltered in  $\Delta$ FIRE mice. This supports the notion that resident macrophages influence cardiac remodeling but recruited macrophages drive infarct size after I/R.

## Transcriptional landscape of resident versus recruited macrophages in I/R injury

To address the differential responses of resident and recruited macrophages to I/R injury, we generated BM chimeric mice. We applied an irradiation-independent model using conditional deletion of *c-myb* to deplete BM hematopoietic cells in CD45.2 mice and replace them with CD45.1 donor HSC. 2 days after I/R injury, we FACS-sorted recruited (CD45.1<sup>+</sup>) and resident (CD45.2<sup>+</sup>) macrophages and carried out bulk RNA sequencing (**Fig 5A** [↗](#)). The two macrophage populations exhibited profound transcriptional differences after I/R injury. Expression of homeostasis-related genes like *Timd4*, *Lyve-1*, *CD163* and *Retnla* was increased in resident CD45.2<sup>+</sup> macrophages (**Fig 5B** [↗](#), **C**). Substantiating the differential regulation of macrophage programs, CD45.1<sup>+</sup> macrophages increased inflammatory- and host defense-related gene ontology (GO) terms (e.g. myeloid leukocyte related immunity, killing of cells), whereas CD45.2<sup>+</sup> macrophages upregulated development- and homeostasis-related GO terms (e.g. extracellular matrix organization, vasculature development, heart muscle development) (**Fig 5D** [↗](#)). GO enrichment analysis further predicted that processes involved in innate (e.g. leukocyte migration, regulation of defense response, response to bacterium) as well as the adaptive immunity (e.g. T cell selection, T cell activation, B cell proliferation) were increased in CD45.1<sup>+</sup> macrophages after infarction (**Fig 5D** [↗](#)). Thus, resident and recruited macrophages provide distinct transcriptional changes and inferred functions in response to I/R.

## Altered inflammatory patterns and immune cell communication in *Csf1r* <sup>$\Delta$ FIRE</sup> mice

To evaluate the immune response of resident and recruited macrophages to I/R injury in  $\Delta$ FIRE mice, we interrogated the transcription profile of CD45<sup>+</sup> cells from the infarct area (**Fig 6A** [↗](#)). In contrast to the absence of homeostatic and antigen-presenting macrophage clusters in healthy hearts of  $\Delta$ FIRE mice (**Fig 2B-C** [↗](#)), there were less differences in immune cell clusters between  $\Delta$ FIRE and control mice 2 days after I/R (**Fig 6B** [↗](#), **C**). Abundance of homeostatic macrophages was also reduced at this time point, however, other clusters including *Ccr2*<sup>hi</sup>*Ly6c*<sup>hi</sup> inflammatory macrophages were not altered, which is in line with our histological findings.

$\Delta$ FIRE was associated with some changes in gene expression in cardiac non-macrophage immune cells. Across different clusters, including lymphocyte and neutrophil clusters, expression of anti-inflammatory genes like *Chil3* (*Ym1*) and *Lcn2* was reduced. Vice versa, expression of Bcl-family genes like *Bcl2a1a* and *Bcl2a1d*, which are associated with apoptosis and inflammatory pathways, was higher in  $\Delta$ FIRE mice (**Fig S6-8**). Other upregulated genes were related to antigen presentation (e.g. *CD74*, *H2-Ab1*), as identified in the *Ccr2*<sup>lo</sup>*Ly6c*<sup>lo</sup>, homeostatic and *Ccr2*<sup>hi</sup>*Ly6c*<sup>hi</sup> macrophage clusters (**Fig S6 and 7**). Further, we interrogated inflammatory gene expression in neutrophils, which are abundant first responders to myocardial infarction. We found that a computed score summing up inflammasome activation (Amorim *et al.*, 2022 [↗](#)) was increased in all neutrophil clusters in  $\Delta$ FIRE mice (**Fig 6D** [↗](#)). Thus, the absence of cardiac macrophages was associated with altered inflammatory properties of non-macrophage immune cells in the infarcted heart.

Altered intercellular crosstalk of macrophages is a hallmark of cardiac inflammation. We therefore assessed ligand-receptor (LR) interactions between immune cell populations after I/R injury. Indeed, the number of LR interactions with neutrophils and lymphocytes, as well as the



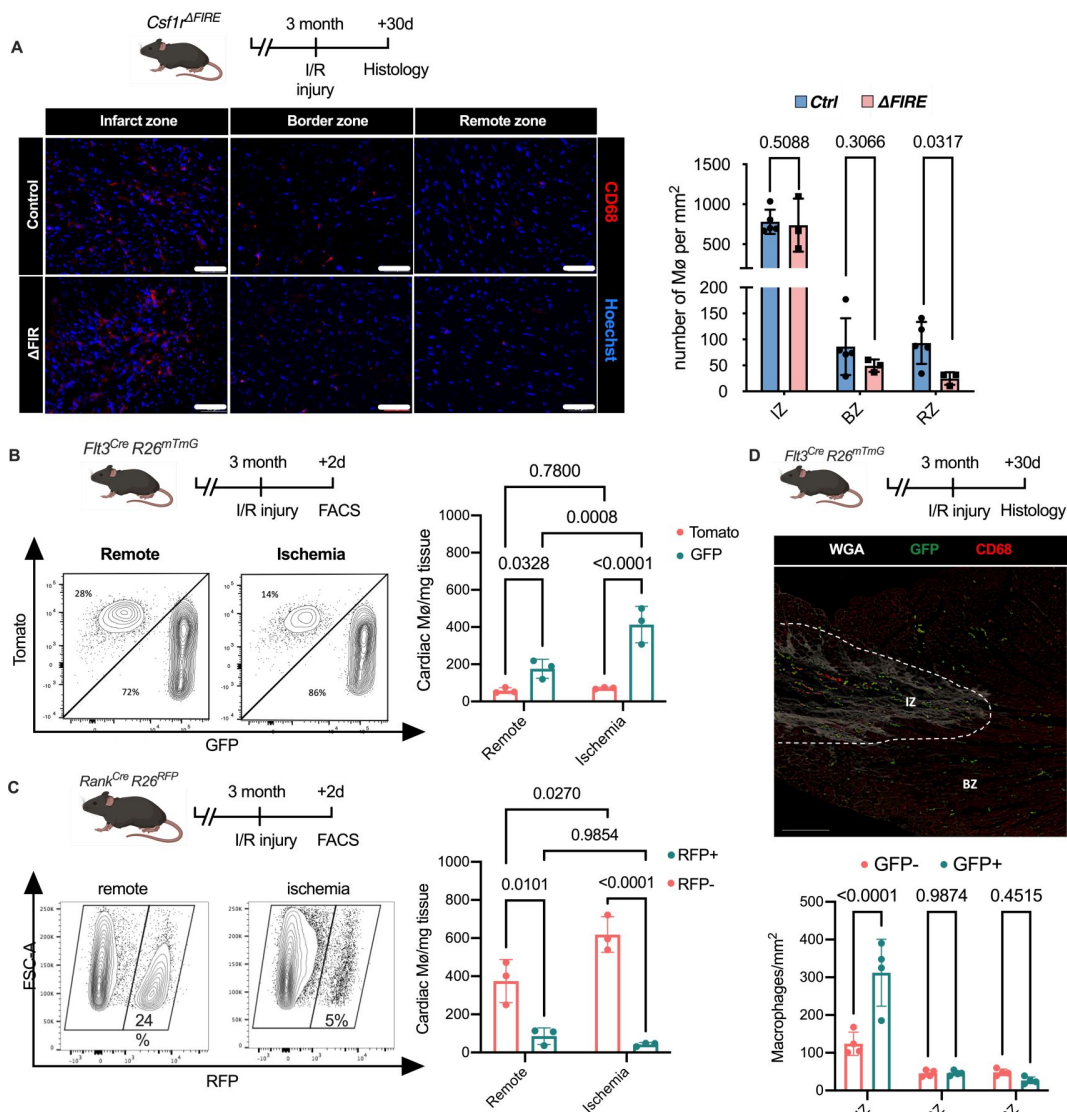


**Figure 4.**

### Recruitment of BM-derived macrophages into infarct zone of *Csf1<sup>ΔFIRE</sup>* mice.

(A) Representative immunohistology of hearts from *ΔFIRE* mice 30 days after I/R injury showing macrophages (CD68<sup>+</sup> cells in red and Hoechst in blue) in the infarct, border and remote zone. Right panel shows number of cardiac macrophages in the respective area (n=5 control and n=3 for *ΔFIRE*). (B) Flow cytometry analysis of *Flt3<sup>Cre</sup>Rosa26<sup>mT/mG</sup>* mice 2 days after I/R injury, (left) representative flow cytometry showing expression of tomato and GFP in macrophages in the remote and ischemic myocardium and (right) number of tomato<sup>+</sup> and GFP<sup>+</sup> cardiac macrophages in the respective area (n=3, each individual experiments). (C) Flow cytometry analysis of *Rank<sup>Cre</sup>Rosa26<sup>RFP</sup>* mice 2 days after I/R injury, (left) representative flow cytometry showing expression of RFP in macrophages in the remote and ischemic myocardium and (right) number of RFP<sup>+</sup> and RFP<sup>-</sup> cardiac macrophages in the respective area (n=3, each individual experiments). (D) Histological analysis of *Flt3<sup>Cre</sup>Rosa26<sup>mT/mG</sup>* mice 30 days after I/R injury in the infarct, border and remote zone, (left) representative immunohistology of the infarct and border zone and (right) number of GFP<sup>+</sup> and GFP<sup>-</sup> cardiac macrophages in the respective areas (n=4). Fishers LSD test was performed for all experiments and mean ± SD is shown.

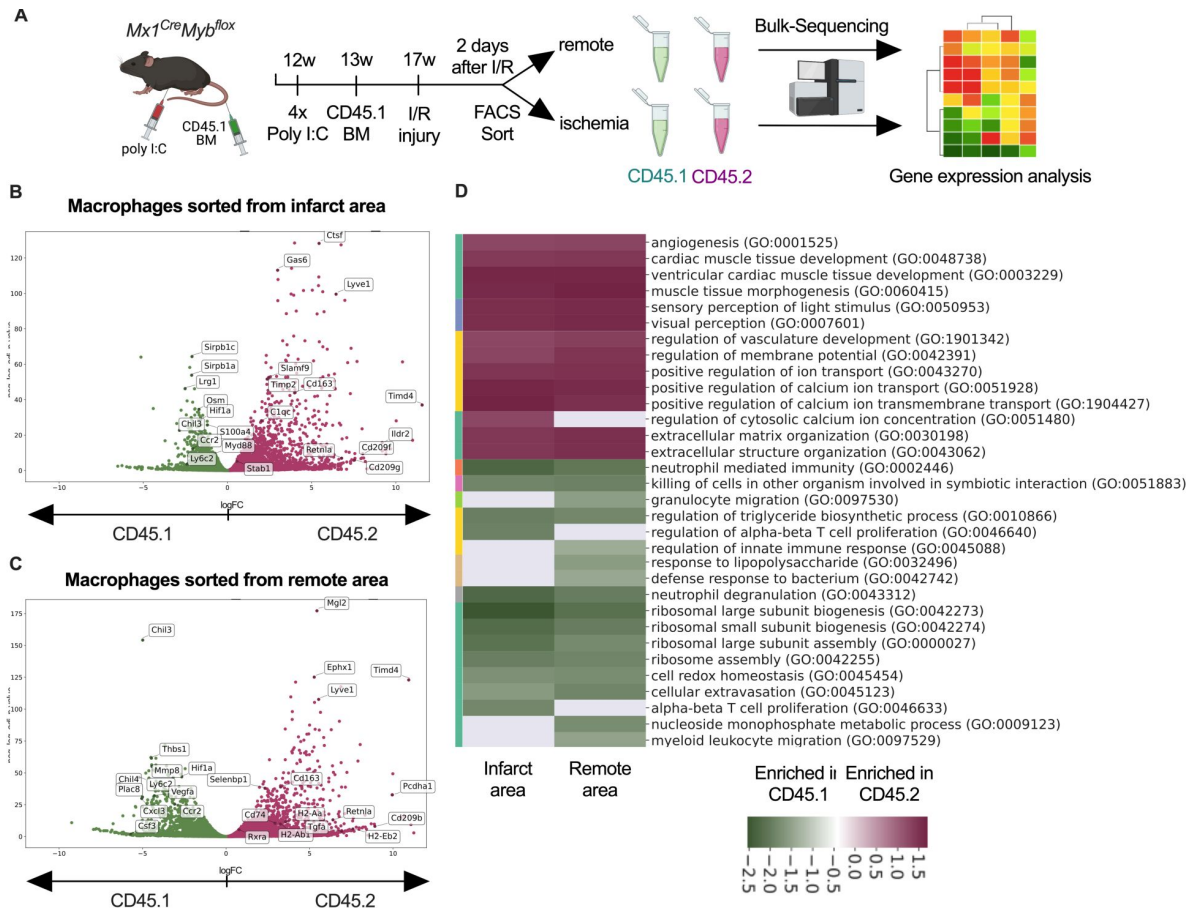


**Figure 5.**

### Transcriptional landscape of resident versus recruited macrophages in I/R injury

**(A)** Experimental setup to generate non-irradiation BM chimera using *CD45.2 Mx1<sup>Cre</sup>Myb<sup>flox/flox</sup>* and transplantation of CD45.1 BM. I/R injury was induced 4 weeks after BM-transplantation and CD45.1<sup>+</sup> and CD45.2<sup>+</sup> macrophages were sorted from the remote and ischemic myocardium 2 days after I/R injury and RNA-sequencing was performed on bulk cells (n=3). **(B and C)** Volcano plot showing differential gene expression analysis results of recruited CD45.1 vs. resident CD45.2 macrophages in the **(B)** remote and **(C)** ischemic zone. **(D)** Gene ontology enrichment analysis showing specific biological processes enriched in CD45.1 and CD45.2 macrophages in the ischemic and remote zone.

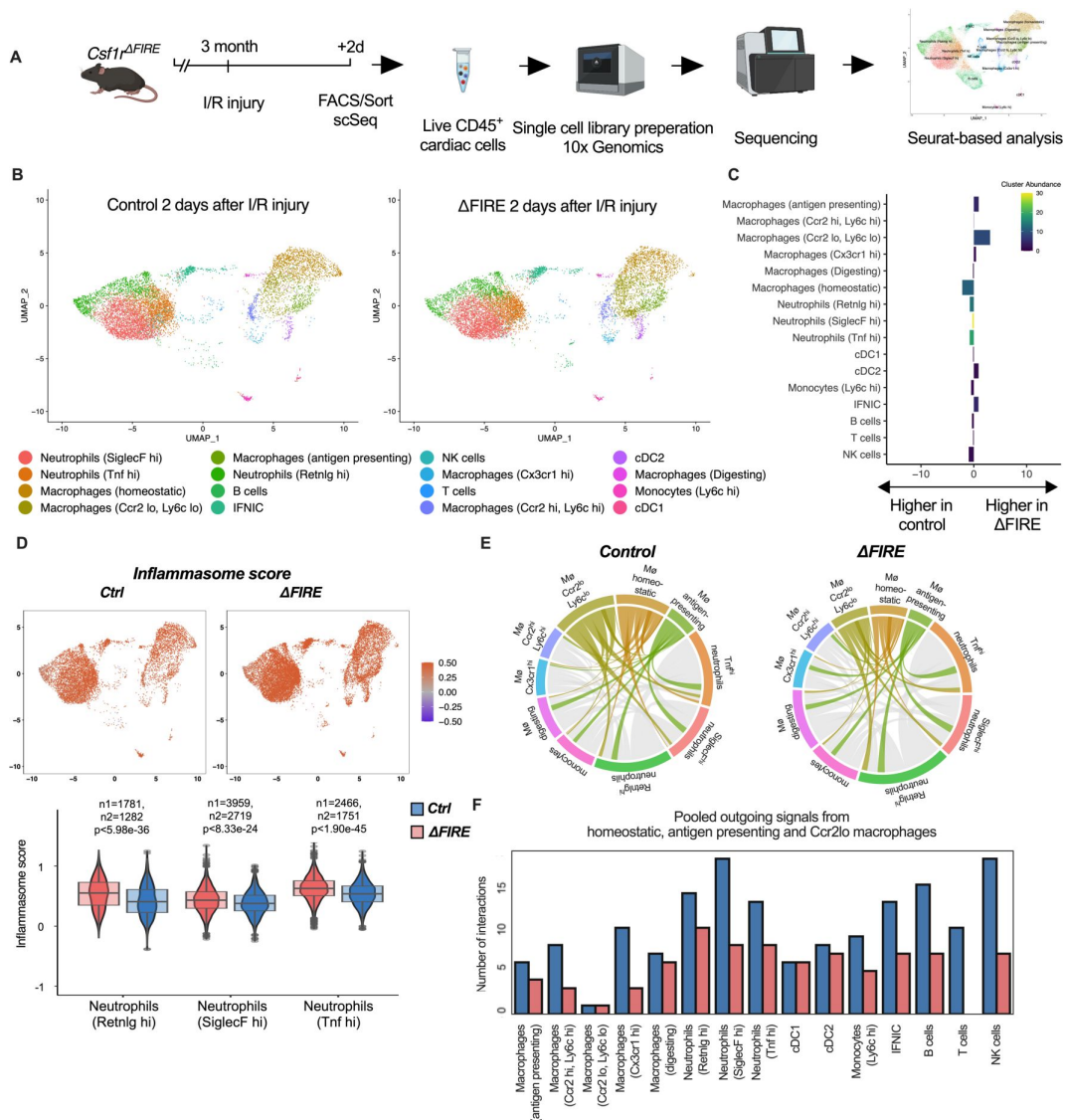


**Figure 6.**

### Altered inflammatory patterns and immune cell communication in *Csfl*<sup>ΔFIRE</sup> mice.

(A) Experimental setup to analyze transcriptional changes in cardiac immune cells on a single cell level 2 days after I/R injury in  $\Delta$ FIRE mice. (B) UMAPs of control and  $\Delta$ FIRE 2 days after I/R injury (n=2 for control and  $\Delta$ FIRE). (C) Absolute difference (percentage points) in cluster abundance between control and  $\Delta$ FIRE. (D) Inflammasome score projected on a UMAP displaying control and  $\Delta$ FIRE immune cell subsets after I/R injury. Violin and box plots show the computed inflammasome score in neutrophil clusters (n1/n2 represents number of cells from control/  $\Delta$ FIRE mice). (E) Ligand-receptor interactions of antigen-presenting, *Ccr2*<sup>lo</sup> *ly6c*<sup>lo</sup> and homeostatic macrophages (highlighted) with other immune cell clusters. Shown are the aggregated communication scores (width of interactions) for all cell types. Only communication scores larger than 6 are considered. (F) Number of interactions (with communication score > 6) outgoing from homeostatic, antigen presenting and *Ccr2*<sup>lo</sup> macrophages to other immune cell clusters.

strength of the macrophage-emitted communication signals was markedly reduced in homeostatic, antigen-presenting and *Ccr2<sup>lo</sup>Ly6c<sup>lo</sup> Mø* macrophage clusters (**Fig 6E**, **F**, **Fig. S9**). In contrast, immune cell communication in BM-derived macrophage clusters (e.g. *Ccr2<sup>hi</sup>Ly6c<sup>hi</sup> Mø cluster*, **Fig S10**) was not different to control mice. Taken together, deficiency in resident macrophages in I/R injury altered the intercellular immune crosstalk and induced a pro-inflammatory signature in e.g. cardiac neutrophils. However, transcriptional profiles of BM-derived inflammatory macrophages were largely unaltered. Together with our histological analysis showing the dominance of recruited BM-derived macrophages in the early phase of I/R, this potentially explained the limited impact of ΔFIRE on functional outcome after I/R injury.

## Ablation of resident and recruited macrophages severely impacts on cardiac healing after I/R injury

To test this hypothesis, we determined the effect of combined ablation of resident and recruited macrophages. We therefore exposed mice to continuous treatment with the CSF1R-inhibitor PLX5622 (**Fig 7A**). In healthy hearts, inhibitor treatment resulted in the absence of cardiac macrophages within 3 days (**Fig S11**). We then subjected mice to I/R injury and investigated outcome by sequential PET imaging and histology (**Fig 7A**). Treatment with PLX5622 diminished macrophage numbers in both remote and infarct areas in the early phase (day 2) after injury. Recruitment of other myeloid cells e.g. neutrophils was not altered in this context (**Fig 7B**). This effect was pronounced in the chronic phase (day 30) after I/R injury, in which macrophages were largely absent in remote, border and infarct zones (**Fig 7C,D**). Absence of resident and recruited macrophages was associated increased infarct size, as determined by fibrosis area (WGA histology) as well as viability defect (PET), and resulted in deterioration of cardiac function (**Fig 7E-I**). Specifically, LVEF was reduced 6 days after I/R, and remained strongly impaired at 30 days (**Fig 7E**).

Taken together, sole absence of resident macrophages had limited negative impact on cardiac remodeling. Absence of both resident and recruited macrophages resulted in a significant increase in infarct size and deterioration of left ventricular function after I/R injury, highlighting a beneficial effect of recruited macrophages in cardiac healing.

## Discussion

Macrophages are key players in cardiac homeostasis and disease (Bajpai *et al.*, 2019; Bajpai *et al.*, 2018; Dick *et al.*, 2019; Epelman *et al.*, 2014; Hulsmans *et al.*, 2017; Nahrendorf *et al.*, 2007; Nicolas-Avila *et al.*, 2020; Panizzi *et al.*, 2010; Sager *et al.*, 2016). The precise understanding of their developmental origin, their functions and their regulation could enable the identification of macrophage-targeted strategies to modify inflammation in the heart. In cardiac repair after myocardial infarction, macrophages have both positive and negative effects. They are critical for tissue repair, angiogenesis, and inflammation regulation, but their actions need to be carefully balanced to prevent excessive inflammation, scar tissue formation, and adverse remodeling. This study sheds light on the differential role of resident and recruited macrophages in cardiac remodeling and outcome after AMI.

BM-derived recruited macrophages represents a small population in the healthy heart but are recruited in vast numbers to the injured myocardium after I/R injury. These recruited cells exhibit substantially different transcriptional profiles in comparison to their resident counterpart, and show pro-inflammatory properties. Resident macrophages remain present in the remote and border zone and display a reparative gene expression profile after I/R injury. In comparison to recruited macrophages, resident macrophages expressed higher levels of genes related to homeostatic functions (e.g. *Lyve-1*, *Timd4*, *CD163*, *Stab1*). These markers have recently been associated with self-renewing tissue macrophages that are maintained independently of BM

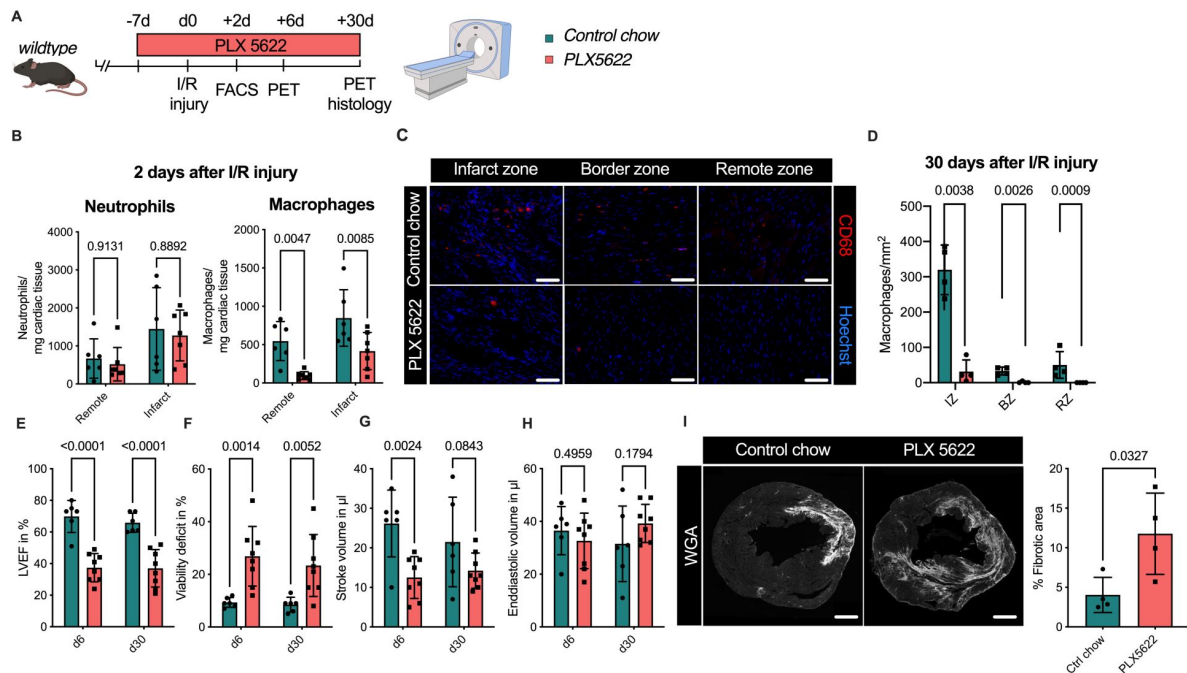


**Figure 7.**

### Ablation of resident and recruited macrophages severely impacts on cardiac healing after I/R injury

**(A)** Schematic of the analysis of cardiac function and infarct size in mice treated with PLX5622 7 days prior and 30 days after I/R injury. **(B)** Number of cardiac macrophages and neutrophils in the remote and ischemic myocardium 2 days after I/R injury in mice fed control chow (n=6) or PLX5622 (n=7). **(C)** Representative immunohistochemistry of hearts 30 days after I/R injury showing macrophages (CD68<sup>+</sup> cells in red and Hoechst in blue) in the infarct, border and remote zone and **(D)** number of cardiac macrophages in the respective area (n=4 for control chow and n=4 for PLX5622). **(E)** Left ventricular ejection fraction (LVEF), **(F)** viability deficit, **(G)** stroke volume and **(H)** end-diastolic volume measured using positron-emission tomography 6 and 30 days after I/R injury (n=6 for control chow, n=8 for PLX5622). **(I)** Representative immunohistochemical images showing the fibrotic area (WGA<sup>+</sup> area) in hearts 30 days after I/R injury from mice fed control chow or PLX5622. Percentage of fibrotic area in the respective groups (n= 4 for each group). Student's t-test or Fishers LSD test was performed and mean  $\pm$  SD is shown.

contribution (Dick *et al.*, 2022 [↗](#)). Biological processes associated with cardiac healing are upregulated in resident macrophages (e.g. regulation of vascular development, regulation of cardiomyocyte development, extracellular matrix organization). Transcriptional profiles of recruited macrophages show enhanced inflammatory biological processes also in macrophages harvested from the remote area, underlining their potentially detrimental influence on remote cardiac injury.

Two recent studies addressed the role of resident macrophages using DT-mediated macrophage depletion and reported impaired cardiac remodeling in chronic myocardial infarction (Dick *et al.*, 2019 [↗](#)) and after I/R injury (Bajpai *et al.*, 2019 [↗](#)). However, DT-mediated cell ablation is known to induce neutrophil recruitment and tissue inflammation (Frieler *et al.*, 2015 [↗](#); Oh *et al.*, 2017 [↗](#); Ruedl & Jung, 2018 [↗](#); Sivakumaran *et al.*, 2016 [↗](#)). This inflammatory preconditioning of cardiac tissue after DT-depletion is likely to impact on cardiac remodeling and influence assessment of tissue macrophage functions. Genomic deletion of FIRE in the *Csf1r* gene results in the near-absence of resident cardiac macrophages but circumvents the inflammatory stimulus of DT-induced depletion.  $\Delta$ FIRE specifically diminished homeostatic and antigen-presenting macrophages. Substantiating the specificity to resident cardiac macrophages in this genetic model, the amount of macrophages recruited to the infarct area after I/R injury was not affected in  $\Delta$ FIRE mice. Further, scRNAseq analysis revealed that gene expression of monocytes as well as *Ccr2<sup>hi</sup>Ly6c<sup>hi</sup>* and *Cx3cr1<sup>hi</sup>* M $\phi$ , representing mainly recruited immune cells, was mostly unchanged in  $\Delta$ FIRE compared to control mice. The specific targeting of the resident macrophage population introduces an interesting *in vivo* model for studying their role in MI without the need for inflammation-prone conditional deletion of macrophages (Frieler *et al.*, 2015 [↗](#)).

Ablation of resident macrophages altered macrophage crosstalk to non-macrophage immune cells, especially lymphocytes and neutrophils. This was characterized by a proinflammatory gene signature, such as neutrophil expression of inflammasome-related genes and a reduction in anti-inflammatory genes like *Chil3* and *Lcn2* (Gordon & Martinez, 2010 [↗](#); Guo *et al.*, 2014 [↗](#); Parmar *et al.*, 2018 [↗](#)). Interestingly, inflammatory polarization of neutrophils have also been associated with poor outcome after ischemic brain injury (Cuartero *et al.*, 2013 [↗](#)). Clinical trials in myocardial infarction patients show a correlation of inflammatory markers with extent of the myocardial damage (Sanchez *et al.*, 2006 [↗](#)) and with short- and long-term mortality (Mueller *et al.*, 2002 [↗](#)).

Our study provides evidence that the absence of resident macrophages negatively influences cardiac remodeling in the late postinfarction phase in  $\Delta$ FIRE mice indicating their biological role in myocardial healing. In the early phase after I/R injury, absence of resident macrophages had no significant effect on infarct size or LV function. These observations potentially indicate a protective role in the chronic phase after myocardial infarction by modulating the inflammatory response, including adjacent immune cells like neutrophils or lymphocytes.

Deciphering in detail the specific functions of resident macrophages is of considerable interest but requires both cell-specific and temporally-controlled depletion of respective immune cells in injury, which to our knowledge is not available at present. These experiments could be important to tailor immune-targeted treatments of myocardial inflammation and postinfarct remodelling.

Depletion of macrophages by pharmacological inhibition of CSF1R induced the absence of both resident and recruited macrophages, allowing us to determine cardiac outcome in juxtaposition to the  $\Delta$ FIRE mice. Continuous CSF1R inhibition induced the absence of macrophages also in the infarcted area and had deleterious effect on infarct size and LV function. In line with our findings, depletion of macrophages by anti-CSF1R treatment was associated with worsened cardiac function in a model of pressure overload induced heart failure (Revelo *et al.*, 2021 [↗](#)). Controversially, a recent study in which monocytes were depleted using DT-injections in *Ccr2<sup>DTR</sup>* mice reported beneficial effects on cardiac outcome after MI in mice (Bajpai *et al.*, 2019 [↗](#)).

An explanation of this controversy might be the timing and duration of macrophage depletion. Bajpai et al. depleted recruited macrophages only in the initial phase of myocardial infarction which improved cardiac healing (Bajpai *et al.*, 2019 [↗](#)), while depletion of macrophages over a longer period of time, as shown in our study, is detrimental for cardiac repair. Further, other immune cells including neutrophils express CCR2 and may therefore be affected directly (Talbot *et al.*, 2015 [↗](#); Xu *et al.*, 2017 [↗](#)). In line with this, Ccr2-deficient mice exhibit reduced acute recruitment of neutrophils to the brain after I/R injury, which was associated with reduced infarct size and brain edema (Dimitrijevic *et al.*, 2007 [↗](#)).

Taken together our study underlines the heterogeneity of cardiac macrophages and the importance of ontogeny therein. Resident macrophages, which mainly derive from YS EMPs, govern cardiac homeostasis in the healthy heart, and contribute positively to cardiac healing after I/R injury by orchestrating anti-inflammatory programming of other cardiac immune cells. However, recruited macrophages contribute to the healing phase after AMI and their absence defines infarct size and cardiac outcome.

## Materials and methods

### Mice

*Rank<sup>Cre</sup>* (Jacome-Galarza *et al.*, 2019 [↗](#); Percin *et al.*, 2018 [↗](#)), *Flt3<sup>Cre</sup>* (Benz *et al.*, 2008 [↗](#)), *Myb<sup>fl/fl</sup>* (Emambokus *et al.*, 2003 [↗](#)), *Mx1<sup>Cre</sup>* (Kuhn *et al.*, 1995 [↗](#)) (from The Jackson Laboratory (JAX), Stock No: 003556), *Csf1r<sup>ΔFIRE</sup>* (Rojo *et al.*, 2019 [↗](#)), *Rosa26<sup>DTR</sup>* (Buch *et al.*, 2005 [↗](#)) (JAX Stock No: 007900), *Rosa26<sup>mT/mG</sup>* (Muzumdar *et al.*, 2007 [↗](#)) (JAX Stock No: 007676), *Rosa26<sup>eYFP</sup>* (Srinivas *et al.*, 2001 [↗](#)) (JAX Stock No: 006148), and *Rosa26<sup>RFP</sup>* (JAX Stock No: 034720) mice have been previously described. PCR genotyping was performed according to protocols described previously. Animals were aged between 10-16 weeks. We have complied with all relevant ethical regulations. Animal studies were approved by the local regulatory agency (Regierung von Oberbayern, Munich, Germany, record numbers ROB-55.2-2532.Vet\_02-19-17 and ROB-55.2-2532.Vet\_02-19-1; Care and Use Committee of the Institut Pasteur (CETEA), dap190119).

FIRE mice were kept on a CBA/Ca background. Experiments in which reporter mice were necessary (*Csf1r<sup>ΔFIRE</sup>Rank<sup>Cre</sup>Rosa26<sup>eYFP</sup>*) the background was mixed with a C57Bl6 background. All experiments evaluating cardiac function and outcome after infarction in FIRE mice were performed on mice kept with a CBA/Ca background.

For fate-mapping analysis of Flt3<sup>+</sup> precursors, *Flt3<sup>Cre</sup>* males (the transgene is located on the Y chromosome) were crossed to *Rosa26<sup>eYFP</sup>* or *Rosa26<sup>mT/mG</sup>* female reporter mice and only the male progeny was used. For all other experiments, the offspring of both sexes was used for experiments.

BM transplantation was enabled by conditional deletion of the transcription factor *myb* as previously described (Stremmel *et al.*, 2018 [↗](#)). In brief, we induced BM ablation by 4 injections of poly:I:C into *CD45.2; Mx1<sup>Cre</sup>Myb<sup>fllox/fllox</sup>* every other day, and then transplanted BM from congenic *C57BL/6 CD45.1 (Ly5.1; JAX Stock No: 006584)*. We confirmed the success (chimerism of above 90%) of the BM-transplantation after 4 weeks.

To deplete macrophages, we used the selective CSF1R-inhibitor PLX5622. Control and PLX5622 (300 ppm formulated in AIN-76A standard chow, Research Diets, Inc.) chows were kindly provided by Plexxikon Inc (Berkeley, CA). For depletion of RANK-lineage macrophages, *Rank<sup>Cre</sup>Rosa26<sup>DTR</sup>* mice were injected intraperitoneally with 0.02 mg/kg body weight diphtheria toxin (DT; Sigma-Aldrich) at the timepoints mentioned in Figure and corresponding legend. Mice were closely monitored by veterinarians and according to score sheets that were approved by the

regulatory agency. Single DT application in *Rank<sup>Cre</sup>Rosa26<sup>DTR</sup>* mice led to rapid deterioration of their health (without infarction or other interventions), and consequently experiments needed to be aborted according to regulations; experimental outcomes were then documented as premature death as indicated.

## Ischemia-reperfusion (I/R) injury

I/R injury was carried out as previously described (Novotny *et al*, 2018 [↗](#)). In brief, mice were anesthetized using 2% isoflurane and intraperitoneal injection of fentanyl (0.05 mg/kg), midazolam (5.0 mg/kg) and medetomidine (0.5 mg/kg), and then intubated orally (MiniVent Ventilator model nr. 845, Harvard Apparatus®) and ventilated (volume of 150  $\mu$ L at 200/min). After lateral thoracotomy, the left anterior descending artery (LAD) was ligated with an 8-0 prolene suture producing an ischemic area in the apical left ventricle (LV). To induce the reperfusion injury, the suture was removed after 60 min and reperfusion was confirmed by observing the recoloring of the LV. Postoperative analgesia was performed by injection of Buprenorphin (0.1 mg/kg) twice per day for 3 days. After 2, 6 or 30 days after I/R injury organs were harvested after cervical dislocation.

## Organ harvest

Mice were anaesthetized using 2% isoflurane and organ harvest was performed after cervical dislocation. Blood was harvested with a heparinized syringe (2mL) by cardiac puncture. After perfusion with 20 mL of ice-cold PBS hearts were excised and kept in PBS on ice until further tissue processing. For flow cytometry, hearts were divided into the ischemia (tissue distal of the LAD ligation) and remote area (tissue proximal of the LAD ligation). For histological examinations of tissues, hearts were incubated in 4% PFA for 30 min followed by an incubation in 30% sucrose-solution (Sigma Aldrich®) for 24 h. Afterwards, hearts were mounted onto a heart slicing device and cut transversally into 3 equal parts (termed level 1, 2 and 3) and stored in Tissue-Tek® (Sakura Finetek Germany GmbH) at <sup>TM</sup>80°C.

## Immunohistology

Cryosections (10-12  $\mu$ m) of heart tissue were fixed with 4% paraformaldehyde for 10 min. Blocking and permeabilization were performed with 0.5% Saponin and 10% goat serum for 1h. Primary antibodies were added and incubated for 2-18 h (see Supplemental Table 1). Slides were washed with PBS and secondary antibodies were added and incubated for 1h (see Supplemental Table 1). WGA-staining (Wheat Germ Agglutinin Alexa Fluor<sup>TM</sup> 647 conjugated antibody, ThermoFisher Scientific®) was used to locate and measure the infarct area and nuclei were stained with DAPI. Finally, slides were washed one more time and Fluorescence Mounting Medium was used to cover the stained sample.

Heart samples were evaluated using an Axio Imager M2 (Carl Zeiss®) and blinded picture analysis was performed using ZEN Imaging and Axiovision SE64 Rel. 4.9.1 (Carl Zeiss®). For the evaluation of cell numbers, 6 individual high-resolution images from each respective anatomical region (infarct area, border zone and remote zone) were analysed for each animal. To measure infarct size the heart was cut into 3 parts and the infarcted area was measured as WGA<sup>+</sup> area in sections from each part.

## Flow cytometry

100  $\mu$ L of heparinized blood was used for FACS analysis. Erythrocytes were lysed with 1% ammonium chloride. After washing with PBS, the cell suspension was resuspended in purified rat anti-mouse CD16/CD32 (BD Pharmingen®) and incubated for 15 min at 4°C. Following this, cells were incubated with FACS-antibodies for 15 min at 4°C (**table S1**).



Heart tissue was dissected into remote and ischemic tissue as described above and minced into small pieces using forceps and a scalpel. When comparing baseline and I/R injury in FACS analysis, basal heart tissue was used for comparison with remote tissue and apical heart tissue for comparison with ischemia tissue. After enzymatic digestion (Collagenase XI 1200 U/mg, Collagenase I 125 U/mg, Hyaluronidase 500 U/mg, DNase I 1836 U/mg; Sigma Aldrich®) for 30 min at 37°C cells were washed and incubated with purified anti-CD16/32 (FcγRIII/II; dilution 1/50) for 10 min. Thereafter, cells were incubated with FACS-antibodies (**table S1**) for 30 min at 4°C. FACS-analysis was performed on a BD Fortessa® or a BeckmanCoulter Cytoflex® flow cytometer and gating strategies are shown in Supplemental Figures 1 and 3. Data were analysed using FlowJo® (version 10.0.8r1).

## Cell Sorting

Cell sorting was performed on a MoFlo Astrios (Beckman Coulter) to obtain cardiac macrophages from *CD45.2; Mx1<sup>Cre</sup>Myb<sup>fllox/fllox</sup>* after BM-transplantation of CD45.1 BM (n=3 for 2 days after I/R injury) for bulk sequencing, or all cardiac immune cells (CD45<sup>+</sup> cells) of *Csf1r<sup>ΔFIRE</sup>* and *Rank<sup>Cre</sup>Rosa26<sup>eYFP</sup>* mice (n=3 for *Csf1r<sup>ΔFIRE/+</sup>* and *Csf1r<sup>ΔFIRE/ΔFIRE</sup>* in baseline conditions, n=1 for *Rank<sup>Cre</sup>Rosa26<sup>eYFP</sup>* in baseline conditions; n=2 for *Csf1r<sup>ΔFIRE/+</sup>* and *Csf1r<sup>ΔFIRE/ΔFIRE</sup>* 2 days after I/R injury) for single cell analysis. CD45<sup>+</sup> cells were enriched by using magnetic beads and MS columns (CD45 MicroBeads; Miltenyi Biotec). Cells were then sorted as single/live/CD45<sup>+</sup> cells for single cell sequencing from baseline hearts and from the ischemic myocardium 2 days after I/R injury. Bulk sequencing was performed on single/live/CD45<sup>+</sup>/lin<sup>-</sup>/CD11b<sup>+</sup>/F4/80<sup>+</sup>/CD64<sup>+</sup>/CD45.1<sup>+</sup> or CD45.2<sup>+</sup> cells from the remote and the ischemic myocardium 2 days after I/R injury. Dead cells were identified with SYTOX Orange Dead Cell Stain.

## Bulk sequencing and analysis

For each sample, ~1000 macrophages were sorted into 75μL of RLT buffer (Qiagen, containing 1% beta-mercaptoethanol), vortexed for 1 min and immediately frozen (-80°C). RNA extraction (RNeasy® Plus Micro Kit, Qiagen), cDNA generation (SMART®-Seq v4 Ultra Low Input RNA Kit, Takara Bio) and library preparation (Nextera® XT DNA Library Prep Kit, Illumina) were performed according to the manufacturer's specifications. Sequencing was performed on a HiSeq4000 system (Illumina).

The obtained reads were trimmed using *bbduk* from the BBMap (<https://sourceforge.net/projects/bbmap/>) v38.87 collection using parameters "ktrim=r k=23 mink=11 hdist=1 tpe tbo". The trimmed reads were aligned with *Hisat2* 2.2.1 against the Ensembl release 102 reference mouse genome (Yates *et al*, 2020 [link](#)).

Gene expression was quantified using the *featureCounts* (Liao *et al*, 2014 [link](#)) application from the subread package (v2.0.1) and with parameters "--primary -O -C -B -p -T 8 --minOverlap 5". Differential expression analysis was performed using *DESeq2* (v1.30.0) (Love *et al*, 2014 [link](#)). A Gene Ontology Set Enrichment analysis was performed using the *ClusterProfiler* R package (v3.18.1). The visualization of the respective clustermaps was layouted using the *ForceAtlas2* implementation of the python *fa2* (<https://pypi.org/project/fa2/>) package for *networkx* (v2.5) (<https://networkx.org/>).

On the library-size normalized count data, the *pymRMR* (Peng *et al*, 2005 [link](#)), (<https://pypi.org/project/pymrnr/>) package was used to derive the top 100 discriminatory genes (Mutual Information Quotient method) for subsequently calculating the UMAP 2D-embedding ((McInnes *et al*, 2020 [link](#)), (<https://pypi.org/project/umap-learn/>)) for all samples (*umap-learn* package v0.5.0rc1, 3 neighbors) ((McInnes *et al*, 2018 [link](#)), (<https://pypi.org/project/pymrnr/>)).

## Single cell RNA sequencing and analysis

After sorting, cells were proceeded for single cell capture, barcoding and library preparation using Chromium Next GEM single cell 3' (v3.1, 10x Genomics) according to manufacturer's specifications. Pooled libraries were sequenced on an Illumina HiSeq1500 sequencer (Illumina, San Diego, USA) in paired-end mode with asymmetric read length of 28+91 bp and a single indexing read of 8bp.

The reads of heart1 sample (*Rank<sup>Cre</sup>Rosa26<sup>eYFP</sup>*) were demultiplexed using Je- demultiplex-illu (Girardot *et al.*, 2016 [↗](#)) and mapped against a customized mouse reference genome (GRCm38.p6, Gencode annotation M24) including eYfp sequence using Cell Ranger (v3.1.0, 10x Genomics).

The six mouse samples 20133-0001 to 20133-0006 (baseline condition of *Csf1r<sup>ΔFIRE/+</sup>* and *Csf1r<sup>ΔFIRE/ΔFIRE</sup>*), were processed using Cellranger 4.0.0 using the 2020A mm10 reference.

The 4 mouse samples (MUC13956-13959, infarct condition of *Csf1r<sup>ΔFIRE/+</sup>* and *Csf1r<sup>ΔFIRE/ΔFIRE</sup>*), were sequenced with 4 technical sequencing replicates and pooled using the cellranger (v4.0.0, 10x Genomics) pipeline. Cellranger 4.0.0 was called with default parameters and the 2020A mm10 reference for gene expression.

Finally, all 11 samples were integrated using Seurat 4.0.0 (on R 4.0.1) (Stuart & Satija, 2019 [↗](#)). The samples were processed, and cells were filtered to contain between 200 and 6000 features, have at least 1000 molecules detected (nCount\_RNA > 1000), have below 15% mtRNA content (^MT) and below 40% ribosomal RNA content (^Rps|^Rpl). After this filtering a total of 35759 cells remained.

After performing SCTransform (Hafemeister & Satija, 2019 [↗](#)) on the samples, the SCTransform vignette for integrating the datasets was followed (with 2000 integration features). For dimensionality reduction, PCA was performed using default parameters, and UMAP and Neighbour-Finding was run on 50 PCs. Clustering was performed at a resolution of 0.8. A total of 18 clusters was identified using this approach. Cluster markers were calculated using the t-test in the FindMarkers function. Subsequently cell types were initially predicted using the cPred cell type prediction ([https://github.com/mjoppich/scrnaseq\\_celltype\\_prediction](https://github.com/mjoppich/scrnaseq_celltype_prediction) [↗](#)). Upon manual curation, further fine-grained cell type annotations were made. Differential comparisons were performed against several subgroups of the data set. These comparisons were performed using the t-test in the FindMarkers function of Seurat. Differential results are visualized using the EnhancedVolcano library (Blighe K, 2021 [↗](#)).

For the analysis of cell-cell interactions we downloaded the ligand-receptor pairs from Jin *et al.* (Jin *et al.*, 2021 [↗](#)) from the Lewis Lab GitHub repository (<https://github.com/LewisLabUCSD/Ligand-Receptor-Pairs> [↗](#)). For each interaction (ligand-receptor pair for a cluster-pair) the communication score is calculated as the expression product (Armingol *et al.*, 2021 [↗](#)) of the mean normalized expressions exported from the Seurat object. This ensures that little expression of either ligand or receptor in only one cluster results in a relatively low communication score, and only good expression of ligand and receptor will result in a high communication score. The direction of an interaction is fixed from ligand to receptor. The single ligand-receptor-communication-scores were then aggregated (sum) such that only interactions with a score greater six were taken into account.

Gene module scores for inflammasome, ROS and phagocytosis gene sets were calculated using Seurat's AddModuleScore function. All scripts, including the ones for creating the visualizations of bulk and scRNA-seq data, are available online through [https://github.com/mjoppich/myocardial\\_infarction](https://github.com/mjoppich/myocardial_infarction) [↗](#).

## In Vivo PET Imaging

ECG-gated positron emission tomography (PET) images were performed on day 6 and 30 after I/R injury of the LAD using a dedicated small-animal PET scanner (Inveon Dedicated PET, Preclinical Solutions, Siemens Healthcare Molecular Imaging, Knoxville, TN, USA), as previously described (Brunner *et al.*, 2012 [↗](#)). Anaesthesia was induced with isoflurane (2.5%), delivered via a face mask in pure oxygen at a rate of 1.2 L/min and maintained with isoflurane (1.5%). Approximately 15 MBq 2-deoxy-2-[18F]fluoro-D-glucose ([18F]-FDG) (~100  $\mu$ L) were administered through a tail vein catheter and slowly flushed immediately afterwards with 50  $\mu$ L saline solution. Body temperature was monitored using a rectal thermometer and maintained within the normal range using a heating pad. After placing animals within the aperture of the PET scanner ECG electrodes (3M, St. Paul, MN, USA) were placed on both forepaws and the left hind paw and ECG was recorded using a dedicated physiological monitoring system (BioVet; Spin Systems Pty Ltd., Brisbane, Australia) (Todica *et al.*, 2018 [↗](#)). The PET emission acquisition (list-mode) was initiated 30 min after [18F]-FDG injection and lasted 15 min (Brunner *et al.*, 2012 [↗](#); Gross *et al.*, 2016 [↗](#)). For scatter and attenuation correction and additional 7-min long transmission scan was performed using a Co-57 source.

The accuracy of the ECG trigger signal was verified retrospectively using in-house software programmed in MATLAB (The Mathworks, Natick, USA) and in C programming language and erroneous trigger events were removed when needed, as previously described (Boning *et al.*, 2013 [↗](#)). Further processing of the data was performed using the Inveon Acquisition Workplace (Siemens Medical Solutions, Knoxville, TN). As previously described, data was reconstructed as a static image or as a cardiac gated image with 16 bins in a  $128 \times 128$  matrix with a zoom of 211% using an OSEM 3D algorithm with 4 and a MAP 3D algorithm with 32 iterations (Brunner *et al.*, 2012 [↗](#)). The reconstructed data was normalized, corrected for randoms, dead time and decay as well as attenuation and scatter.

PET images were analysed using the Inveon Research Workplace in a blinded manner (Siemens Medical Solutions, Knoxville, TN). Infarct sizes were determined from static reconstructed images using QPS® (Cedars-Sinai, Los Angeles, CA, USA). Hereby, datasets were compared to a normative database and the viability defect was calculated as percentage of the left ventricular volume, as described previously (Lehner *et al.*, 2014 [↗](#); Todica *et al.*, 2014 [↗](#)). Left ventricular function volumes (EDV, ESV, SV), as well as the LVEF, were determined from ECG-gated images using QGS® (Cedars-Sinai, Los Angeles, CA, USA), as described previously (Brunner *et al.*, 2012 [↗](#); Croteau *et al.*, 2003 [↗](#)).

## Statistical analysis

Student's t-test or Fisher's LSD test was used (Prism GraphPad®). Welch's correction for unequal variances was used when applicable. A p-value of  $p < 0.05$  was considered significant. The Shapiro-Wilk test was used to test normality. Data are presented as mean  $\pm$  standard deviation (SD).

## Acknowledgements

We thank Nicole Blount, Beate Jantz, Michael Lorenz, Sebastian Helmer for excellent technical assistance.

## Funding

DZHK (German Centre for Cardiovascular Research) and the BMBF (German Ministry of Education and Research) (grants 81Z0600204 to CS, 81 $\times$ 2600252 to TW and 81 $\times$ 2600256 to MF). The Deutsche Forschungsgemeinschaft (SCHU 2297/1-1 and collaborative research centers 1123 project Z02 (MJ,

RZ) and A07 (CS), and CRC TRR332 project A6 (CS). LMUexcellent (TW). ESC Research Grant 2021 (TW). Friedrich-Baur Stiftung (TW). Deutsche Stiftung für Herzforschung (M.F.). Chinese Scholarship Council (CSC) to JF and LL.

## Author contributions

Conceptualization: TW, CSchu

Methodology: TW, MJ, MF, JL, GP, AT, DE, CSchu

Investigation: TW, DM, MJ, MF, CG, KK, VW, SR, SA, JF, LL, WHL, JW, LT, DE, GP, SMS

Funding acquisition: TW, MF, RZ, EGP, CSchu Supervision: AH, CW, SE, AT, RZ, CP, EGP, CSchu

Writing – original draft: TW, MJ

Writing – review & editing: all authors

## Conflict of interest

The authors declare no conflict of interest.

## Conflict-of-interest statement

The authors have declared that no conflict of interest exists.

## References

- Ahmad FB, Anderson RN (2021) **The Leading Causes of Death in the US for 2020** *JAMA*
- Amorim A *et al.* (2022) **IFN $\gamma$  and GM-CSF control complementary differentiation programs in the monocyte-to-phagocyte transition during neuroinflammation** *Nat Immunol* **23**:217–228
- Armingol E, Officer A, Harismendy O, Lewis NE (2021) **Deciphering cell-cell interactions and communication from gene expression** *Nat Rev Genet* **22**:71–88
- Bajpai G *et al.* (2019) **Tissue Resident CCR2- and CCR2+ Cardiac Macrophages Differentially Orchestrate Monocyte Recruitment and Fate Specification Following Myocardial Injury** *Circ Res* **124**:263–278
- Bajpai G *et al.* (2018) **The human heart contains distinct macrophage subsets with divergent origins and functions** *Nat Med* **24**:1234–1245
- Benz C, Martins VC, Radtke F, Bleul CC (2008) **The stream of precursors that colonizes the thymus proceeds selectively through the early T lineage precursor stage of T cell development** *J Exp Med* **205**:1187–1199
- Blighe KRS, Lewis M (2021) **EnhancedVolcano: Publication-ready volcano plots with enhanced colouring and labeling** *R package version 1.10.0*
- Boning G, Todica A, Vai A, Lehner S, Xiong G, Mille E, Ilhan H, la Fougere C, Bartenstein P, Hacker M (2013) **Erroneous cardiac ECG-gated PET list-mode trigger events can be retrospectively identified and replaced by an offline reprocessing approach: first results in rodents** *Phys Med Biol* **58**:7937–7959
- Brunner S *et al.* (2012) **Left ventricular functional assessment in murine models of ischemic and dilated cardiomyopathy using [18 F]FDG-PET: comparison with cardiac MRI and monitoring erythropoietin therapy** *EJNMMI Res* **2**
- Buch T, Heppner FL, Tertilt C, Heinen TJ, Kremer M, Wunderlich FT, Jung S, Waisman A (2005) **A Cre-inducible diphtheria toxin receptor mediates cell lineage ablation after toxin administration** *Nat Methods* **2**:419–426
- Croteau E, Benard F, Cadorette J, Gauthier ME, Aliaga A, Bentourkia M, Lecomte R (2003) **Quantitative gated PET for the assessment of left ventricular function in small animals** *J Nucl Med* **44**:1655–1661
- Cuartero MI, Ballesteros I, Moraga A, Nombela F, Vivancos J, Hamilton JA, Corbi AL, Lizasoain I, Moro MA (2013) **N2 neutrophils, novel players in brain inflammation after stroke: modulation by the PPAR $\gamma$  agonist rosiglitazone** *Stroke* **44**:3498–3508
- Dick SA *et al.* (2019) **Self-renewing resident cardiac macrophages limit adverse remodeling following myocardial infarction** *Nat Immunol* **20**:29–39
- Dick SA *et al.* (2022) **Three tissue resident macrophage subsets coexist across organs with conserved origins and life cycles** *Sci Immunol* **7**

Dimitrijevic OB, Stamatovic SM, Keep RF, Andjelkovic AV (2007) **Absence of the chemokine receptor CCR2 protects against cerebral ischemia/reperfusion injury in mice** *Stroke* **38**:1345–1353

Emambokus N, Vegiopoulos A, Harman B, Jenkinson E, Anderson G, Frampton J (2003) **Progression through key stages of haemopoiesis is dependent on distinct threshold levels of c-Myb** *EMBO J* **22**:4478–4488

Epelman S *et al.* (2014) **Embryonic and adult-derived resident cardiac macrophages are maintained through distinct mechanisms at steady state and during inflammation** *Immunity* **40**:91–104

Frieler RA *et al.* (2015) **Depletion of macrophages in CD11b diphtheria toxin receptor mice induces brain inflammation and enhances inflammatory signaling during traumatic brain injury** *Brain Res* **1624**:103–112

Gerber Y, Weston SA, Enriquez-Sarano M, Berardi C, Chamberlain AM, Manemann SM, Jiang R, Dunlay SM, Roger VL (2016) **Mortality Associated With Heart Failure After Myocardial Infarction: A Contemporary Community Perspective** *Circ Heart Fail* **9**

Ginhoux F *et al.* (2010) **Fate mapping analysis reveals that adult microglia derive from primitive macrophages** *Science* **330**:841–845

Girardot C, Scholtalbers J, Sauer S, Su SY, Furlong EE (2016) **Je, a versatile suite to handle multiplexed NGS libraries with unique molecular identifiers** *BMC Bioinformatics* **17**

Perdigueró E Gomez *et al.* (2015) **Tissue-resident macrophages originate from yolk-sac-derived erythro-myeloid progenitors** *Nature* **518**:547–551

Gordon S, Martinez FO (2010) **Alternative activation of macrophages: mechanism and functions** *Immunity* **32**:593–604

Gross L *et al.* (2016) **FDG-PET reveals improved cardiac regeneration and attenuated adverse remodelling following Sitagliptin + G-CSF therapy after acute myocardial infarction** *Eur Heart J Cardiovasc Imaging* **17**:136–145

Guo H, Jin D, Chen X (2014) **Lipocalin 2 is a regulator of macrophage polarization and NF-kappaB/STAT3 pathway activation** *Mol Endocrinol* **28**:1616–1628

Hafemeister C, Satija R (2019) **Normalization and variance stabilization of single-cell RNA-seq data using regularized negative binomial regression** *Genome Biol* **20**

Heidt T *et al.* (2014) **Differential contribution of monocytes to heart macrophages in steady-state and after myocardial infarction** *Circ Res* **115**:284–295

Hilgendorf I *et al.* (2014) **Ly-6Chigh monocytes depend on Nr4a1 to balance both inflammatory and reparative phases in the infarcted myocardium** *Circ Res* **114**:1611–1622

Honold L, Nahrendorf M (2018) **Resident and Monocyte-Derived Macrophages in Cardiovascular Disease** *Circ Res* **122**:113–127

Hulsmans M *et al.* (2017) **Macrophages Facilitate Electrical Conduction in the Heart** *Cell* **169**:510–522

Jacome-Galarza CE *et al.* (2019) **Developmental origin, functional maintenance and genetic rescue of osteoclasts** *Nature* **568**:541–545

Jin S, Guerrero-Juarez CF, Zhang L, Chang I, Ramos R, Kuan CH, Myung P, Plikus MV, Nie Q (2021) **Inference and analysis of cell-cell communication using CellChat** *Nat Commun* **12**

Kubota A, Suto A, Suzuki K, Kobayashi Y, Nakajima H (2019) **Matrix metalloproteinase-12 produced by Ly6C(low) macrophages prolongs the survival after myocardial infarction by preventing neutrophil influx** *J Mol Cell Cardiol* **131**:41–52

Kuhn R, Schwenk F, Aguet M, Rajewsky K (1995) **Inducible gene targeting in mice** *Science* **269**:1427–1429

Lehner S *et al.* (2014) **In vivo monitoring of parathyroid hormone treatment after myocardial infarction in mice with [68Ga]annexin A5 and [18F]fluorodeoxyglucose positron emission tomography** *Mol Imaging* **13**:1–8

Liao Y, Smyth GK, Shi W (2014) **featureCounts: an efficient general purpose program for assigning sequence reads to genomic features** *Bioinformatics* **30**:923–930

Love MI, Huber W, Anders S (2014) **Moderated estimation of fold change and dispersion for RNA-seq data with DESeq2** *Genome Biol* **15**

Lozano R *et al.* (2012) **Global and regional mortality from 235 causes of death for 20 age groups in 1990 and 2010: a systematic analysis for the Global Burden of Disease Study 2010** *Lancet* **380**:2095–2128

Mass E *et al.* (2016) **Specification of tissue-resident macrophages during organogenesis** *Science* **353**

McInnes L, Healy J, Melville J (2020) **UMAP: Uniform Manifold Approximation and Projection for Dimension Reduction** *arXiv*

McInnes L, Healy J, Saul N, Großberger L (2018) **UMAP: Uniform Manifold Approximation and Projection** *J Open Source Softw* **3**

Mueller C, Buettner HJ, Hodgson JM, Marsch S, Perruchoud AP, Roskamm H, Neumann FJ (2002) **Inflammation and long-term mortality after non-ST elevation acute coronary syndrome treated with a very early invasive strategy in 1042 consecutive patients** *Circulation* **105**:1412–1415

Munro DAD, Bradford BM, Mariani SA, Hampton DW, Vink CS, Chandran S, Hume DA, Pridans C, Priller J (2020) **CNS macrophages differentially rely on an intronic Csf1r enhancer for their development** *Development* **147**

Muzumdar MD, Tasic B, Miyamichi K, Li L, Luo L (2007) **A global double-fluorescent Cre reporter mouse** *Genesis* **45**:593–605

Nahrendorf M, Swirski FK, Aikawa E, Stangenberg L, Wurdinger T, Figueiredo JL, Libby P, Weissleder R, Pittet MJ (2007) **The healing myocardium sequentially mobilizes two monocyte subsets with divergent and complementary functions** *J Exp Med* **204**:3037–3047

Nicolas-Avila JA *et al.* (2020) **A Network of Macrophages Supports Mitochondrial Homeostasis in the Heart** *Cell* **183**:94–109

Novotny J *et al.* (2018) **Histological comparison of arterial thrombi in mice and men and the influence of Cl-amidine on thrombus formation** *PLoS one* **13**

Oh DS, Oh JE, Jung HE, Lee HK (2017) **Transient Depletion of CD169(+) Cells Contributes to Impaired Early Protection and Effector CD8(+) T Cell Recruitment against Mucosal Respiratory Syncytial Virus Infection** *Front Immunol* **8**

Panizzi P, Swirski FK, Figueiredo JL, Waterman P, Sosnovik DE, Aikawa E, Libby P, Pittet M, Weissleder R, Nahrendorf M (2010) **Impaired infarct healing in atherosclerotic mice with Ly-6C(hi) monocytosis** *J Am Coll Cardiol* **55**:1629–1638

Parmar T, Parmar VM, Perusek L, Georges A, Takahashi M, Crabb JW, Maeda A (2018) **Lipocalin 2 Plays an Important Role in Regulating Inflammation in Retinal Degeneration** *J Immunol* **200**:3128–3141

Peng H, Long F, Ding C (2005) **Feature selection based on mutual information: criteria of max-dependency, max-relevance, and min-redundancy** *IEEE Trans Pattern Anal Mach Intell* **27**:1226–1238

Percin GI, Eitler J, Kranz A, Fu J, Pollard JW, Naumann R, Waskow C (2018) **CSF1R regulates the dendritic cell pool size in adult mice via embryo-derived tissue-resident macrophages** *Nat Commun* **9**

Revelo X, Parthiban P, Chen C, Barrow F, Fredrickson G, Wang H, Yucel D, Herman A, van Berlo JH (2021) **Cardiac Resident Macrophages Prevent Fibrosis and Stimulate Angiogenesis** *Circ Res*

Rojo R *et al.* (2019) **Deletion of a Csf1r enhancer selectively impacts CSF1R expression and development of tissue macrophage populations** *Nat Commun* **10**

Ruedl C, Jung S (2018) **DTR-mediated conditional cell ablation-Progress and challenges** *Eur J Immunol* **48**:1114–1119

Sager HB *et al.* (2016) **Proliferation and Recruitment Contribute to Myocardial Macrophage Expansion in Chronic Heart Failure** *Circ Res* **119**:853–864

Sanchez PL, Rodriguez MV, Villacorta E, Albarran C, Cruz I, Moreiras JM, Martin F, Pabon P, Fernandez-Aviles F, Martin-Luengo C (2006) **[Kinetics of C-reactive protein release in different forms of acute coronary syndrome]** *Rev Esp Cardiol* **59**:441–447

Schulz C *et al.* (2012) **A lineage of myeloid cells independent of Myb and hematopoietic stem cells** *Science* **336**:86–90

Sivakumaran S *et al.* (2016) **Depletion of CD11c(+) cells in the CD11c.DTR model drives expansion of unique CD64(+) Ly6C(+) monocytes that are poised to release TNF-alpha** *Eur J Immunol* **46**:192–203

Srinivas S, Watanabe T, Lin CS, Williams CM, Tanabe Y, Jessell TM, Costantini F (2001) **Cre reporter strains produced by targeted insertion of EYFP and ECFP into the ROSA26 locus** *BMC Dev Biol* **1**

Stremmel C *et al.* (2018) **Inducible disruption of the c-myc gene allows allogeneic bone marrow transplantation without irradiation** *J Immunol Methods* **457**:66–72



Stuart T, Satija R (2019) **Integrative single-cell analysis** *Nat Rev Genet* **20**:257–272

Talbot J *et al.* (2015) **CCR2 Expression in Neutrophils Plays a Critical Role in Their Migration Into the Joints in Rheumatoid Arthritis** *Arthritis Rheumatol* **67**:1751–1759

Todica A, Beetz NL, Gunther L, Zacherl MJ, Grabmaier U, Huber B, Bartenstein P, Brunner S, Lehner S (2018) **Monitoring of Cardiac Remodeling in a Mouse Model of Pressure-Overload Left Ventricular Hypertrophy with [(18)F]FDG MicroPET** *Mol Imaging Biol* **20**:268–274

Todica A *et al.* (2014) **In-vivo monitoring of erythropoietin treatment after myocardial infarction in mice with [(6)(8)Ga]Annexin A5 and [(1)(8)F]FDG PET** *J Nucl Cardiol* **21**:1191–1199

Weinberger T *et al.* (2020) **Ontogeny of arterial macrophages defines their functions in homeostasis and inflammation** *Nat Commun* **11**

Weinberger T, Schulz C (2015) **Myocardial infarction: a critical role of macrophages in cardiac remodeling** *Front Physiol* **6**

Xu P, Zhang J, Wang H, Wang G, Wang CY, Zhang J (2017) **CCR2 dependent neutrophil activation and mobilization rely on TLR4-p38 axis during liver ischemia-reperfusion injury** *Am J Transl Res* **9**:2878–2890

Yates AD *et al.* (2020) **Ensembl 2020** *Nucleic Acids Res* **48**:D682–D688

Zaman R, Epelman S (2022) **Resident cardiac macrophages: Heterogeneity and function in health and disease** *Immunity* **55**:1549–1563

## Article and author information

### Tobias Weinberger

Medical Clinic I., Department of Cardiology, University Hospital, Ludwig Maximilian University, 81377 Munich, Germany, Institute of Surgical Research at the Walter-Brendel-Centre of Experimental Medicine, University Hospital, Ludwig Maximilian University, 81377 Munich, Germany, DZHK (German Centre for Cardiovascular Research), partner site Munich Heart Alliance, 80336 Munich, Germany, Institut Pasteur, Unité Macrophages et Développement de l'Immunité, Département de Biologie du Développement et Cellules Souches, Paris, France

### Denise Messerer

Medical Clinic I., Department of Cardiology, University Hospital, Ludwig Maximilian University, 81377 Munich, Germany, Institute of Surgical Research at the Walter-Brendel-Centre of Experimental Medicine, University Hospital, Ludwig Maximilian University, 81377 Munich, Germany

### Markus Joppich

LFE Bioinformatik, Department of Informatics, Ludwig Maximilian University, 80333 Munich, Germany  
ORCID iD: [0000-0002-6665-8951](https://orcid.org/0000-0002-6665-8951)

**Max Fischer**

Medical Clinic I., Department of Cardiology, University Hospital, Ludwig Maximilian University, 81377 Munich, Germany, Institute of Surgical Research at the Walter-Brendel-Centre of Experimental Medicine, University Hospital, Ludwig Maximilian University, 81377 Munich, Germany, DZHK (German Centre for Cardiovascular Research), partner site Munich Heart Alliance, 80336 Munich, Germany  
ORCID iD: [0000-0001-9172-3316](https://orcid.org/0000-0001-9172-3316)

**Clarisabel Garcia**

Institut Pasteur, Unité Macrophages et Développement de l'Immunité, Département de Biologie du Développement et Cellules Souches, Paris, France

**Konda Kumaraswami**

Medical Clinic I., Department of Cardiology, University Hospital, Ludwig Maximilian University, 81377 Munich, Germany, Institute of Surgical Research at the Walter-Brendel-Centre of Experimental Medicine, University Hospital, Ludwig Maximilian University, 81377 Munich, Germany

**Vanessa Wimpler**

Medical Clinic I., Department of Cardiology, University Hospital, Ludwig Maximilian University, 81377 Munich, Germany, Institute of Surgical Research at the Walter-Brendel-Centre of Experimental Medicine, University Hospital, Ludwig Maximilian University, 81377 Munich, Germany

**Sonja Ablinger**

Medical Clinic I., Department of Cardiology, University Hospital, Ludwig Maximilian University, 81377 Munich, Germany, Institute of Surgical Research at the Walter-Brendel-Centre of Experimental Medicine, University Hospital, Ludwig Maximilian University, 81377 Munich, Germany

**Saskia Räuber**

Medical Clinic I., Department of Cardiology, University Hospital, Ludwig Maximilian University, 81377 Munich, Germany, Institute of Surgical Research at the Walter-Brendel-Centre of Experimental Medicine, University Hospital, Ludwig Maximilian University, 81377 Munich, Germany, Department of Neurology, Medical Faculty, Heinrich Heine University of Düsseldorf, 40225 Düsseldorf, Germany  
ORCID iD: [0000-0001-8901-5572](https://orcid.org/0000-0001-8901-5572)

**Jiahui Fang**

Medical Clinic I., Department of Cardiology, University Hospital, Ludwig Maximilian University, 81377 Munich, Germany, Institute of Surgical Research at the Walter-Brendel-Centre of Experimental Medicine, University Hospital, Ludwig Maximilian University, 81377 Munich, Germany

**Lulu Liu**

Medical Clinic I., Department of Cardiology, University Hospital, Ludwig Maximilian University, 81377 Munich, Germany, Institute of Surgical Research at the Walter-Brendel-Centre of Experimental Medicine, University Hospital, Ludwig Maximilian University, 81377 Munich, Germany

**Wing Han Liu**

Medical Clinic I., Department of Cardiology, University Hospital, Ludwig Maximilian University, 81377 Munich, Germany

**Julia Winterhalter**

Medical Clinic I., Department of Cardiology, University Hospital, Ludwig Maximilian University, 81377 Munich, Germany, Institute of Surgical Research at the Walter-Brendel-Centre of Experimental Medicine, University Hospital, Ludwig Maximilian University, 81377 Munich, Germany

**Johannes Lichti**

Medical Clinic I., Department of Cardiology, University Hospital, Ludwig Maximilian University, 81377 Munich, Germany

**Lukas Tomas**

Medical Clinic I., Department of Cardiology, University Hospital, Ludwig Maximilian University, 81377 Munich, Germany, Institute of Surgical Research at the Walter-Brendel-Centre of Experimental Medicine, University Hospital, Ludwig Maximilian University, 81377 Munich, Germany, DZHK (German Centre for Cardiovascular Research), partner site Munich Heart Alliance, 80336 Munich, Germany

**Dena Esfandyari**

DZHK (German Centre for Cardiovascular Research), partner site Munich Heart Alliance, 80336 Munich, Germany, Institute of Pharmacology and Toxicology, Technical University Munich, 80802 Munich, Germany

**Guelce Percin**

Immunology of Aging, Leibniz-Institute on Aging - Fritz-Lipmann-Institute (FLI), 07745 Jena, Germany

**Sandra Martin Salamanca**

Area of Cell & Developmental Biology, Centro Nacional de Investigaciones Cardiovasculares Carlos III, Madrid, Spain

**Andres Hidalgo**

Area of Cell & Developmental Biology, Centro Nacional de Investigaciones Cardiovasculares Carlos III, Madrid, Spain, Vascular Biology and Therapeutics Program and Department of Immunobiology, Yale University School of Medicine, New Haven, CT, USA

**Claudia Waskow**

Immunology of Aging, Leibniz-Institute on Aging - Fritz-Lipmann-Institute (FLI), 07745 Jena, Germany, Faculty of Biological Sciences, Friedrich-Schiller-University, 07737 Jena, Germany  
ORCID iD: [0000-0003-3261-0922](https://orcid.org/0000-0003-3261-0922)

**Stefan Engelhardt**

DZHK (German Centre for Cardiovascular Research), partner site Munich Heart Alliance, 80336 Munich, Germany, Institute of Pharmacology and Toxicology, Technical University Munich, 80802 Munich, Germany  
ORCID iD: [0000-0001-5378-8661](https://orcid.org/0000-0001-5378-8661)

**Andrei Todica**

Department of Nuclear Medicine, Ludwig Maximilian University, 81377 Munich, Germany

**Ralf Zimmer**

LFE Bioinformatik, Department of Informatics, Ludwig Maximilian University, 80333 Munich, Germany

**Clare Pridans**

University of Edinburgh Centre for Inflammation Research, The Queen's Medical Research Institute, Edinburgh EH16 4TJ, United Kingdom, Simons Initiative for the Developing Brain, Centre for Discovery Brain Sciences, University of Edinburgh, Edinburgh EH8 9XD, United Kingdom

**Elisa Gomez-Perdiguero**

Institut Pasteur, Unité Macrophages et Développement de l'Immunité, Département de Biologie du Développement et Cellules Souches, Paris, France

ORCID iD: [0000-0002-7717-7897](https://orcid.org/0000-0002-7717-7897)

**Christian Schulz**

Medical Clinic I., Department of Cardiology, University Hospital, Ludwig Maximilian University, 81377 Munich, Germany, Institute of Surgical Research at the Walter-Brendel-Centre of Experimental Medicine, University Hospital, Ludwig Maximilian University, 81377 Munich, Germany, DZHK (German Centre for Cardiovascular Research), partner site Munich Heart Alliance, 80336 Munich, Germany

**For correspondence:** [Christian.schulz@med.un-muenchen.de](mailto:Christian.schulz@med.un-muenchen.de)

**Copyright**

© 2023, Weinberger et al.

This article is distributed under the terms of the [Creative Commons Attribution License](https://creativecommons.org/licenses/by/4.0/), which permits unrestricted use and redistribution provided that the original author and source are credited.

**Editors**

Reviewing Editor

**Florent Ginhoux**

Singapore Immunology Network, Singapore, Singapore

Senior Editor

**Olujimi Ajijola**

University of California, Los Angeles, Los Angeles, United States of America

**Reviewer #1 (Public Review):**

Weinberger et al. use different fate-mapping models, the FIRE model and PLX-diet to follow and target different macrophage populations and combine them with single-cell data to understand their contribution to heart regeneration after I/R injury. This question has already been addressed by other groups in the field using different models. However, the major strength of this manuscript is the usage of the FIRE mouse model that, for the first time, allows specific targeting of only fetal-derived macrophages.

The data show that the absence of resident macrophages is not influencing infarct size but instead is altering the immune cell crosstalk in response to injury, which is in line with the current idea in the field that macrophages of different origins have distinct functions in tissues, especially after an injury.

To fully support the claims of the study, specific targeting of monocyte-derived macrophages or the inhibition of their influx at different stages after injury would be of high interest.

In summary, the study is well done and important for the field of cardiac injury. But it also provides a novel model (FIRE mice + RANK-Cre fate-mapping) for other tissues to study the function of fetal-derived macrophages while monocyte-derived macrophages remain intact.

<https://doi.org/10.7554/eLife.89377.3.sa1>

### **Reviewer #2 (Public Review):**

In this study Weinberger et al. investigated cardiac macrophage subsets after ischemia/reperfusion (I/R) injury in mice. The authors studied a  $\Delta$ FIRE mouse model (deletion of a regulatory element in the *Csf1r* locus), in which only tissue resident macrophages might be ablated. The authors showed a reduction of resident macrophages in  $\Delta$ FIRE mice and characterized its macrophages populations via scRNAseq at baseline conditions and after I/R injury. 2 days after I/R protocol  $\Delta$ FIRE mice showed an enhanced pro inflammatory phenotype in the RNAseq data and differential effects on echocardiographic function 6 and 30 days after I/R injury. Via flow cytometry and histology the authors confirmed existing evidence of increased bone marrow-derived macrophage infiltration to the heart, specifically to the ischemic myocardium. Macrophage population in  $\Delta$ FIRE mice after I/R injury were only changed in the remote zone. Further RNAseq data on resident or recruited macrophages showed transcriptional differences between both cell types in terms of homeostasis-related genes and inflammation. Depleting all macrophage using a *Csf1r* inhibitor resulted in a reduced cardiac function and increased fibrosis.

Strengths:

- (1) The authors utilized robust methodology encompassing state of the art immunological methods, different genetic mouse models and transcriptomics.
- (2) The topic of this work is important given the emerging role of tissue resident macrophages in cardiac homeostasis and disease.

Comments on revised version:

The authors have responded to all questions. I have no further comments and congratulate the authors on their work.

<https://doi.org/10.7554/eLife.89377.3.sa0>

### **Author Response**

The following is the authors' response to the previous reviews.

#### ***Recommendations for the authors:***

#### ***Reviewer #1 (Recommendations For The Authors):***

*The authors have addressed most of the points that were made. However, despite some things that may well be beyond the scope, I would like to insist on a few small points:*

*Point 1: If the authors have conducted a gross analysis of cardiac morphology by histology already, they should include this data in the manuscript and comment with 1-2 sentences that "cardiac healing"... "is unlikely influenced by developmental defects".*

We agree with the reviewer that this analysis is important. Therefore, we are currently conducting an in-depth analysis of the cardiac phenotype of different mouse strains lacking distinct subpopulations of cardiac macrophages in development and non-stimulated (baseline) conditions, including functional, metabolic and even electrophysiological aspects. These analysis will also include FIRE mice. While a gross analysis in this mouse strain did not show pathologic aspects, we look forward to the very detailed tissue characterization before publishing any data from a first basic analysis.

*Point 7: There is still no legend in Figure 6: what is read? What is blue?*

We added the respective legend in the figure.

*Point 8: Please add the information on the background of mice used for the different FIRE mice into the methods part of the paper*

We added the information in the Methods Part (lines 344-347).

**Reviewer #2 (Recommendations For The Authors):**

*The authors have responded to all questions. I have no further comments and congratulate the authors on their work.*

We thank the reviewer for their important questions and the constructive feedback.